Specific Targeting of Peripheral Serotonin 5-HT$_3$ Receptors. Synthesis, Biological Investigation, and Structure−Activity Relationships

Elena Morelli,[II,⊥] Sandra Gemma,[II,§] Roberta Budriesi,[#] Giuseppe Campiani,*[,II,§] Ettore Novellino,[II,⊥] Caterina Fattorusso,[II,†] Bruno Catalanotti,[II,†] Salvatore Sanna Coccone,[II,§] Sindu Ros,[II,§] Giuseppe Borrelli,[II,§] Vinod Kumar,[II,§] Marco Persico,[II,†] Isabella Fiorini,[II,§] Vito Nacci,[II,§] Pierfranco Ioan,[#] Alberto Chiarini,[#] Michel Hamon,[‡] Alfredo Cagnotto,[II,∞] Tiziana Mennini,[II,∞] Claudia Fracasso,[II,∞] Milena Colovic,[II,∞] Silvio Caccia,[II,∞] and Stefania Butini[II,§]

European Research Centre for Drug Discovery and Development, Banchi di Sotto 55, 53100 Siena, Italy, Dipartimento Farmaco Chimico Tecnologico, Università di Siena, Via Aldo Moro 53100 Siena, Italy, Dipartimento di Chimica delle Sostanze Naturali (DCSN) e Dipartimento di Chimica Farmaceutica e Tossicologica (DCFT), Università di Napoli "Federico II", Via D. Montesano 49, 80131 Napoli, Italy, Dipartimento di Scienze Farmaceutiche, Università di Bologna, Via Belmeloro 6, 40126 Bologna, Italy, Neurobiologie Cellulaire et Functionnelle, Istitut National de la Santé et de la Recherche Medicale (INSERM) U. 677, Facultè de Medicine Pitie-Salpetriere 91, Boulevard de l'Hopital, 75634 Paris, Cedex 13, France, and Istituto di Ricercha Farmacologiche Mario Negri, Via La Masa 19, 20156 Milano, Italy

Received September 25, 2008

The synthesis and the biological characterization of novel highly selective pyrroloquinoxaline 5-HT$_3$ receptor (5-HT$_3$R) ligands are described. In functional and in vivo biological studies the novel quinoxalines modulated cardiac parameters by direct interaction with myocardial 5-HT$_3$Rs. The potent 5-HT$_3$R ligands **4h** and **4n** modulate chronotropy (right atrium) but not inotropy (left atrium) at the cardiac level, being antagonist and partial agonist, respectively. Preliminary pharmacokinetic studies indicate that (*S*)-**4n** and **4a**, representatives of the novel 5-HT$_3$R ligands, possess poor blood−brain barrier permeability, being the prototypes of peripherally acting 5-HT$_3$R modulators endowed with a clear-cut pharmacological activity at the cardiac level. The unique properties of **4h** and **4n**, compared to their previously described centrally active *N*-methyl analogue **5a**, are mainly due to the hydrophilic groups at the distal piperazine nitrogen. These analogues represent novel pharmacological tools for investigating the role of peripheral 5-HT$_3$R in the modulation of cardiac parameters.

Introduction

Serotonin (5-HT[a]) is a neurotransmitter involved in many biological and pathological processes. Among the seven major families of 5-HT receptors only the 5-HT$_3$ receptor (5-HT$_3$R) is a pentameric ligand-gated ion channel, and it belongs to the Cys-loop family.[1] The 5-HT$_3$R has attracted much attention as a therapeutic target, since its antagonists are effective in preventing emesis induced by treatment with chemotherapeutic drugs. On the contrary, the potential therapeutic relevance of 5-HT$_3$R agonists is still unclear.[2] Many studies indicate heterogeneous properties for this receptor which could be explained on the basis of different subunit composition. To date, five subunits, 5-HT3A−E,[3] have been identified and cloned showing differences in both the amino terminal and the transmembrane region.[4−6] These subunits are coassembled in homomeric or heteromeric receptor subtypes differing in localization and functions.[4] Furthermore, there is evidence of two splice variants of 5-HT3A: the short and the long isoforms.[7] Expression of splice variants and subunits is different in the central nervous system (CNS) and in peripheral tissues.[8] The presence of intraspecies differences would have a great impact, not least because selective interaction with individual 5-HT$_3$R subtypes may offer increased therapeutic benefits.

The role of 5-HT$_3$R in peripheral tissues has not been widely investigated. Modulation of cardiac function by 5-HT through 5-HT$_3$R is highly intriguing, and development of peripheral 5-HT$_3$R ligands (agonists or antagonists) still remains a challenge and might lead to novel cardiomodulators. The cardiovascular effects of 5-HT are mediated by a direct interaction with three main types of receptors, the so-called 5-HT$_1$-like, 5-HT$_2$R, and 5-HT$_3$R, and by modulation of the cholinergic neurotransmission at the cardiac level.[9] 5-HT can produce a tachycardic effect mediated by activation of 5-HT$_3$R, with positive inotropic and chronotropic effects, mimicked by the agonist quipazine (**1**, Chart 1) and by 2-Me-5-HT (**2**).[10] Recently, the cardiovascular profile of a 5-HT$_3$R agonist (YM-31636, **3**) was reported. However, positive chronotropic effects of **3** were accompanied by potent agonist activity on intestinal receptors (5-HT$_4$R, colon water secretion) and on neuronal 5-HT$_3$Rs.[11]

In order to exploit the intriguing therapeutic potential of modulating peripheral 5-HT$_3$R, the aim of the present study was the development of novel and selective 5-HT$_3$R ligands targeting peripheral cardiac receptors possibly lacking behavioral effects. Because of the lack of structural information relative to Cys-loop receptors that could drive the design strategy of peripheral 5-HT$_3$R modulators, we exploited our previous experience in the field.[12,13] Accordingly, we decided of achieving "peripheral" selectivity by modulating the

* To whom correspondence should be addressed. Phone: 0039-0577-234172. Fax: 0039-0577-234333. E-mail: campiani@unisi.it.
[II] European Research Centre for Drug Discovery and Development.
[⊥] DCFT, Università di Napoli.
[§] Università di Siena.
[#] Università di Bologna.
[†] DCSN, Università di Napoli.
[‡] Istitut National de la Santé et de la Recherche Medicale.
[∞] Istituto di Ricerche Farmacologiche Mario Negri.

[a] Abbreviations: 5-HT, serotonin; 5-HT$_3$R, 5-HT$_3$ receptor; CNS, central nervous system; BBB, blood−brain barrier; von B-J, von Bezold−Jarish; CDI, *N*,*N*-carbonyldiimidazole; DBU, 1,8-diazabicyclo[5.4.0]undec-7-ene; MM, molecular mechanics; PBG, 1-phenylbiguanide; IS, internal standard; DIPEA, *N*,*N*-diisopropylethylamine; DCM, dichloromethane; THF, tetrahydrofuran; *N*,*N*-DMF, *N*,*N*-dimethylformamide; CV, coefficients of variation; PSS, physiological salt solution; DMSO, dimethyl sufoxide.

10.1021/jm900018b CCC: $40.75
Published on Web 05/08/2009

Chart 1. Reference and Title Compounds

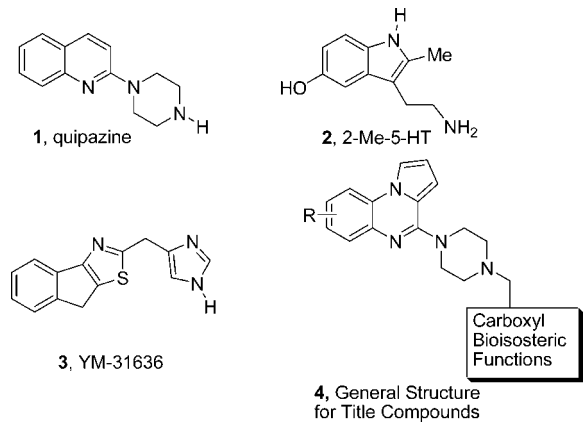

Chart 2. Potent 5-HT$_3$ Receptor Ligands Previously Described

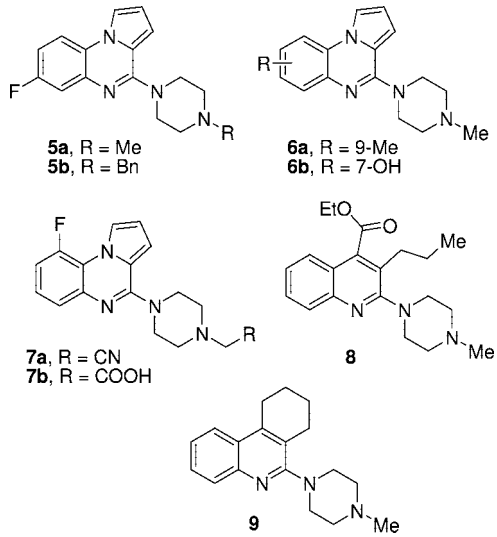

physical−chemical properties of our previously developed arylpiperazine 5-HT$_3$R selective ligands, thus preventing their crossing of the blood−brain barrier (BBB). With this aim, we designed pyrroloquinoxalines (**4**) characterized by different pK_a values and endowed with high affinity and selectivity for 5-HT$_3$R. Most of the quipazine-like 5-HT$_3$R ligands so far reported by our group (**5**−**7**)[12,13] and by others (**8**[14] and **9**,[15] Chart 2) were characterized by different substituents at the piperazine N-4 position and at the polycyclic system. Thus, we report herein the development of novel pyrroloquinoxalines that combine specific substituents at the benzo-fused system (7-F, 9-Me, 7-OH) to key "acidic" (**4a**−**f**,**h**−**n**, Table 1) or polar (**4g** and **4o**, Table 1) functions at piperazine the N-4 position. We also explored the effect of carboxyl bioisosterism. The selected functional groups differ in their charge distribution, in the number and the position of their H-bonding groups, and in steric hindrance. Explored functions are represented by carboxylic group (**4a** and **4b**), amide (**4c**), hydroxamic acid (**4d** and **4e**), *N*-hydroxyimidamide (**4h**), alcoholic (**4g**), sulfonylamide (**4j**), heterocyclic azoles (**4i**, **4k**, and **4l**), oxadiazolone (**4m**), α-amino acid (**4n**). Their 5-HT$_3$R occupancy was evaluated by in vitro binding (Table 1). A set of potent and selective 5-HT$_3$R ligands were used in functional studies for assessing their capability of modulating cardiac parameters and were tested in vivo on the von Bezold−Jarish (von B-J) reflex test. In addition, brain to plasma concentrations of **4n** and **4a** were measured after systemic injection.

Chemistry

As shown in Schemes 1−3, the synthesis of compounds **4a**−**o** was accomplished starting from our previously described piperazinylpyrroloquinoxalines **10a**−**c** by standard functional group transformations.[13] Intermediates **11a**−**d** (Scheme 1) were obtained by *N*-alkylation of the **10a**−**c** piperazine N-4, using suitable 2-bromoacetyl esters. These latter represent key intermediates for the synthesis of **4a**,**b**,**d**,**e**,**j**,**m**. The free acids **4a**,**b** (Scheme 1) were obtained by catalytic hydrogenation of the corresponding benzyl esters **11c**,**d**. From **10a**, treatment with 2-bromoacetonitrile provided the intermediate **12** that, after exposure to potassium hydroxide, afforded **4c**. Ethyl esters **11a**,**b** were treated with hydroxylamine to afford the corresponding hydroxyacetamides **4d**,**e**. Alkylation of **10a** with 2-bromophenylacetic acid ethyl ester afforded an ester intermediate that was hydrolyzed to obtain **4f** or reduced to give **4g**. Treatment of **4a** with methanesulfonamide in the presence of *N*,*N*-carbonyldiimidazole (CDI) and 1,8-diazabicyclo[5.4.0]undec-7-ene (DBU) furnished **4j** (Scheme 2). Exposure of intermediate **12** (obtained form **10a**) to hydroxylamine or sodium azide afforded **4h** and **4k**, respectively. For the synthesis of **4i** and **4l**, compound **10a** was heated in the presence of *N*-formyl-2-chloroacetamidohydrazone (**4i**) or *N*-carbomethoxy-2-chloroacetamidohydrazone (**4l**).[16] Compound **11a** was converted into **4m** through a two step procedure involving the synthesis of a hydrazido intermediate obtained by exposure of **11a** to hydrazine, followed by cyclization with CDI.

For the synthesis of **4n** (Scheme 3) the introduction of the alkyl chain was performed by using (*R*)- or (*S*)-3-[(*tert*-butoxycarbonyl)amino]oxetan-2-one, in turn prepared from (*R*)- or (*S*)-serine. This latter acted as chiral electrophilic alanine cation equivalent that reacted with the nucleophiles and provided optically pure alanine derivatives.[17] Compound **4o** was synthesized by a coupling reaction between **10a** and *N*-Boc-serine in the presence of 1-hydroxybenzotriazole. The resulting intermediate (*S*)-**13** was deprotected by exposure to trifluoroacetic acid to afford (*S*)-**4o** in good overall yield.

Quipazine derivative **15** (Scheme 4) was easily obtained from **1** by alkylation (**14**) followed by saponification (**15**).

Biological Assays. The 5-HT$_3$R affinity of the new compounds was assessed in binding studies given in Table 1. A subset of compounds were further examined for their selectivity toward serotonin (5-HT$_{1A}$R, 5-HT$_{2A}$R, and 5-HT$_4$R), adrenergic (α_1 and α_2), dopamine (DA$_1$ and DA$_2$), and muscarinic receptors (Table 2). The tested compounds did not show affinity up to 10 μM, except compounds (*S*)- and (*R*)-**4n**, which showed a submicromolar affinity for 5-HT$_{1A}$R with no stereoselectivity of interaction.

5-HT$_3$R efficacy was measured by functional assays in guinea pig myocardium and aortic strips (Table 3). In vivo studies were performed on several new compounds on the von B-J reflex test (Table 4). Additionally, brain and plasma concentrations were simultaneously measured for a subset of ligands after systemic injection (Figure 4).

Molecular Modeling. In order to define the pharmacophoric features of our new series of arylpiperazine ligands, we performed a 3D structure−activity relationship (SAR) analysis taking into account previously reported pharmacophoric and receptor models for 5-HT$_3$R[14,18−37] (Table 1 of Supporting Information (SI) and Figure 1 of SI). For this goal, compounds **4a**−**o** (Table 1) were subjected to computational studies in order

Table 1. 5-HT_3R Binding Affinities (K_i, nM), Tautomers, Percentage of Ionic Forms, Clusters, and Single pK_a Values of Compounds **1**, **4a**−**o**, **5a**,**b**, **6a**,**b**, and **15**

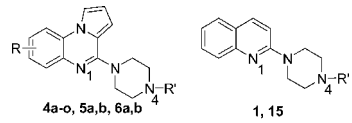

Compd	Tautomer (T)	R	R'	Ionic Form (%)[a]	Cluster	K_i[b] (± SEM)	Single pK_a[c]		
							N-1	*N*-4	R'[d]
4a		7-F	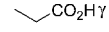	A(14) ZW(86)	A	11.7 (1.0)	3.6	4.4	4.5 (γ)
4b		7-OH	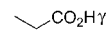	A(18) ZW(82)	A	2.1 (0.4)	4.7	4.4	4.6 (γ) 8.0[e]
4c		7-F	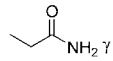	N(100)	B	7.3 (2.2)	3.6	4.5	16.3 (γ)
4d	T1	7-F	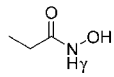	N(100)	B	2.2 (0.3)	3.6	4.4	10.4 (γ)
	T2		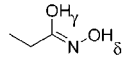	N(100)		-	3.6	4.1	9.5 (γ) 12.7 (δ)
4e	T1	9-Me	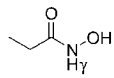	N(99) P(1)	B	3.0 (0.5)	5.1	4.5	10.4 (γ)
	T2		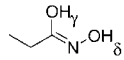	N(99) P(1)		-	5.1	4.2	9.5 (γ) 12.7 (δ)
(±)-4f		9-Me	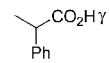	A(59) ZW(41)	A	44 (10)	5.1	4.1	4.0 (γ)
(±)-4g		9-Me	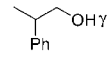	N(98) P(2)	B	79 (15)	5.1	5.3	14.6 (γ)
4h	T1	7-F	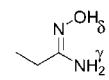	N(84) P(16)	B	0.8 (0.2)	3.6	4.8	12.9 (δ) 6.7 (γ)
	T2		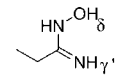	N(92) P(8)		-	3.6	4.8	11.1 (δ) 8.2 (γ')
4i	T1	7-F	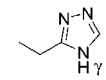	N(100)	B	3.4 (0.04)	3.0	4.4	10.8 (γ)
	T2		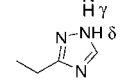	N(100)			3.0	4.4	10.8 (δ)
4j		7-F	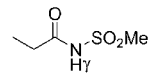	A(100)	-	246 (27)	3.6	4.1	4.3 (γ)
4k		7-F	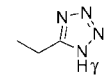	A(68) ZW(32)	A	65 (8)	3.0	2.9	4.9 (γ)
4l	T1	7-F	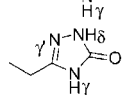	N(93) A(7)	B	17 (1.7)	3.6	4.6	6.0 (γ) 8.5 (γ') 9.5 (δ)
	T2		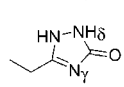	N(93) P(7)		-	3.0	3.6	9.7 (δ) 6.0 (γ')
	T3		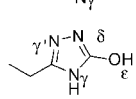	N(73) A(28)		-	3.0	4.1	10.1 (γ') 7.5 (ε) 3.0 (γ)
	T4		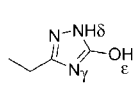	N(69) A(31)		-	2.9	4.1	10.5 (δ) 7.5 (ε) 3.0 (γ)
4m	T1	7-F	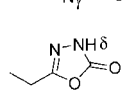	A(45) ZW(55)	A	127 (13)	3.6	4.9	6.9 (δ)
	T2		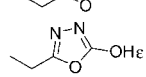	A(100)		-	3.6	4.9	4.7 (ε)
(*S*)-**4n**		7-F	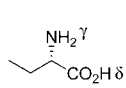	ZW(97) P(3)	B	2.8 (0.3)	3.6	5.5	4.0 (δ) 7.5 (γ)

Table 1. Continued

Compd	Tautomer (T)	R	R'	Ionic Form (%)[a]	Cluster	K_i[b] (± SEM)	Single pK_a[c] N-1	N-4	R'[d]
(*R*)-**4n**		7-F	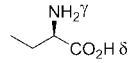	-	B	1.2 (0.2)	-	-	-
4o		7-F	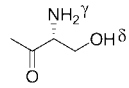	N(6) P(94)	B	237 (21)	3.6	0.1	7.5 (γ)
15		-	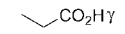	A(7) ZW(90) P(3)		11.2 (1.6)	6.6	4.7	4.5 (γ)
1			H	N(5) P(94) 2P(1)		0.96 (0.11)	6.6	8.9	-
5a		7-F	Me	N(48) P(52)		0.8 (0.05)[f]	3.6	7.2	-
5b		7-F	CH_2Ph	N(96) P(4)		13 (3)[g]	3.6	5.8	-
6a		9-Me	Me	N(45) P(55)		0.8 (0.1)[g]	5.1	7.4	-
6b		7-OH	Me	A(2) ZW(50) P(48)		0.7 (0.1)[g]	4.7	7.3	8.0[e]

[a] Percentage of the ionic forms derived from apparent pK_a values: A = anionic; N = neutral; P = protonated; ZW = zwitterionic (ACD/Labs V10.0, Toronto, Canada). [b] K_i in nM. Each value is the mean ± SEM of three determinations and represent the concentration giving half-maximal inhibition of [^{3}H]LY278584 binding to rat cortical homogenate. [c] ACD/Labs V10.0, Toronto, Canada. [d] The ionizable function is specified in parentheses by the position of the heteroatom with respect to N-4. [e] Ionization of 7-OH substituent. [f] From ref 12. [g] From ref 13.

Scheme 1. Synthesis of Compounds **4a**−**g**

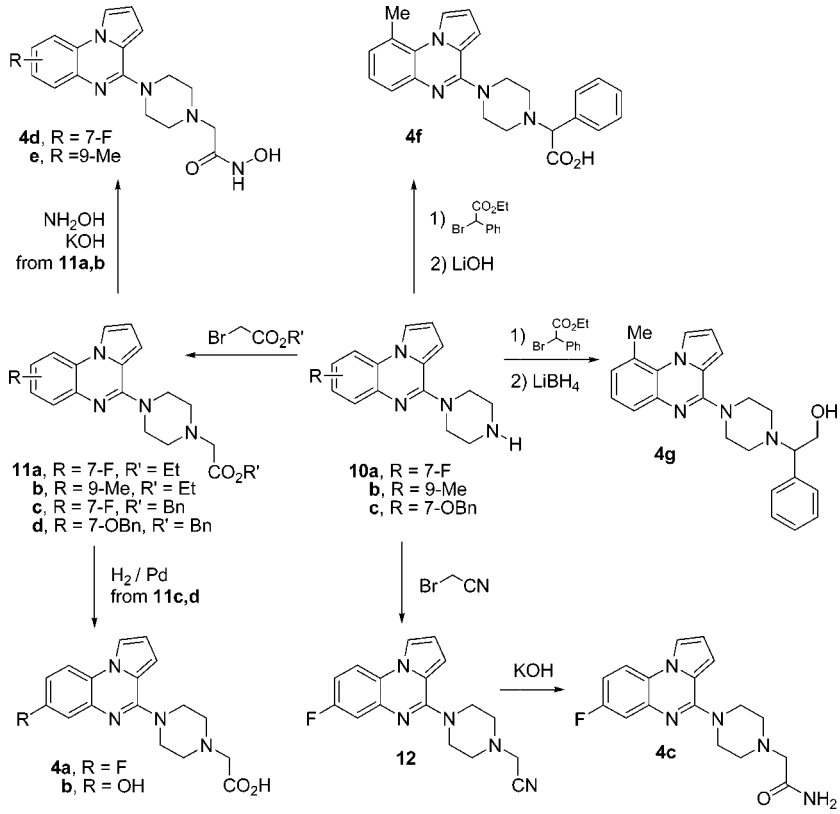

to analyze their conformational and electronic behavior. Different calculation methods were used (see Experimental Section for details) for properly describing the **4a**−**o** extended π system and piperazine N-4 substituents (in equilibrium among different ionizable tautomeric forms). First, **4a**−**o** tautomers were modeled in their most abundant ionic form at pH 7.2, according to calculated pK_a values (Table 1). The conformational space was then sampled by means of a simulated annealing procedure

Scheme 2. Synthesis of Compounds **4h**−**m**

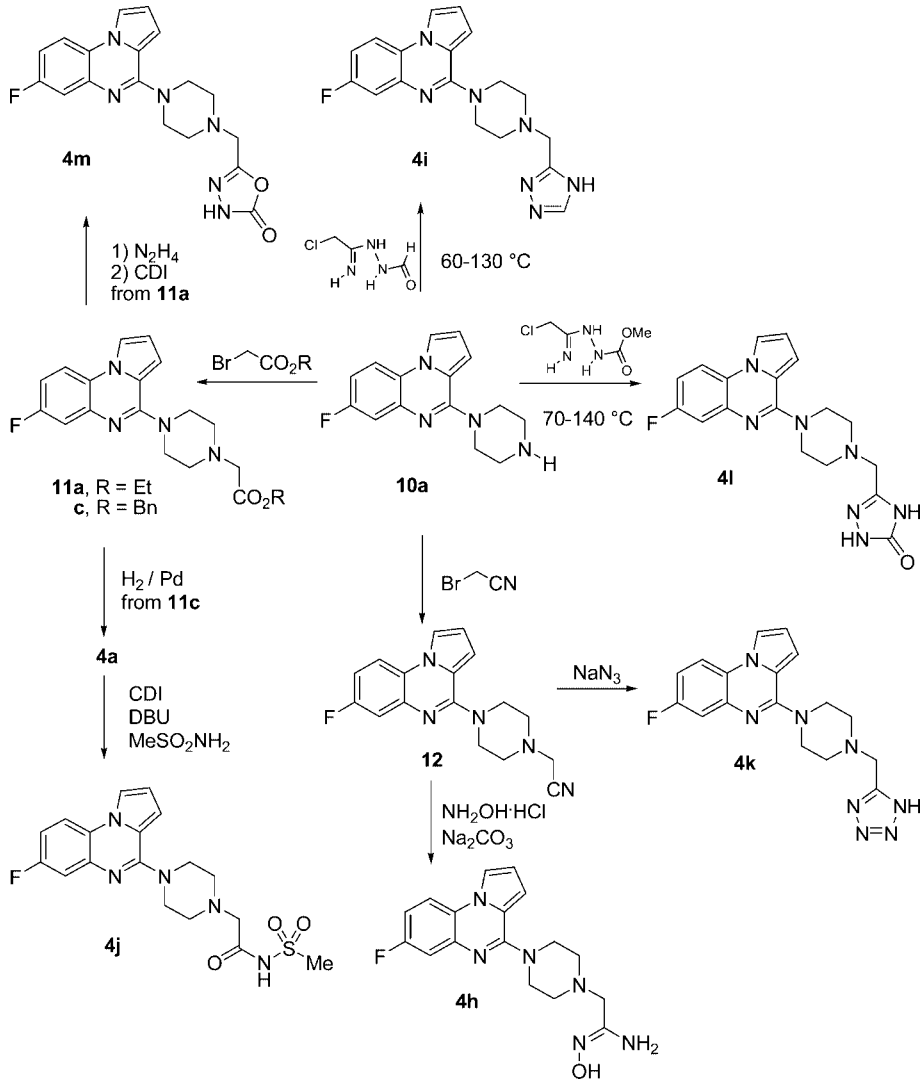

Scheme 3. Synthesis of Compounds **4n**−**o**

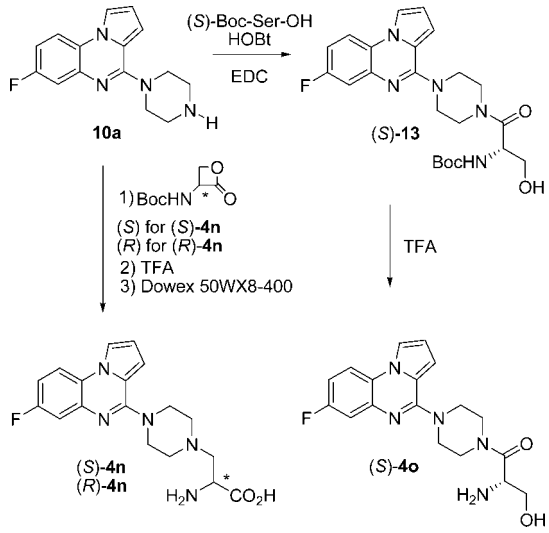

followed by molecular mechanics (MM) geometry optimization using the dielectric constant of water ($\varepsilon = 80r$) to simulate the conformational behavior in aqueous solution. Resulting conformers were grouped into families according to geometric features (see Experimental Section) and ranked by their conformational energy. In order to widen structure selection for successive semiempirical (AM1) geometry optimization, MM conformers' energy was also evaluated by performing a single point (1-SCF) AM1 calculation. The MM global minimum energy conformer of each compound and the 1-SCF lowest energy conformer of each family were selected for successive full geometry optimization by using AM1 semiempirical method (performed in vacuum). Finally, Coulson and ESP partial charges of AM1 conformers were calculated either with AM1 or with MNDO semiempirical methods.

Scheme 4. Synthesis of Compound **15**

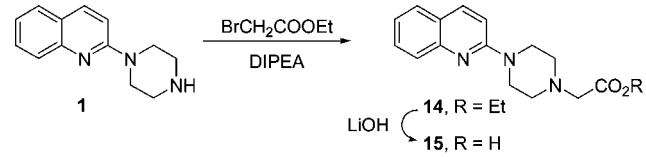

Fully optimized AM1 conformers were resubjected to structural classification into families in the frame of previously reported pharmacophoric models of 5-HT_3R ligands.[14,18] These latter conformers are characterized by the presence of a total positive net charge on the molecule and by the correct orientation of three key pharmacophoric groups: (i) a protonated nitrogen, (ii) an H-bond acceptor (carbonyl oxygen or hetero-

Table 2. Binding Profile of Selected Compounds on a Panel of Neurotransmitter Receptors

	K_i [a] (±SEM), nM							
compd	5-HT$_{1A}$ [b]	5-HT$_{2A}$ [c]	5-HT$_4$ [d]	α_{1NA} [e]	α_{2NA} [f]	DA$_1$ [g]	DA$_2$ [h]	muscarinic [i]
4h	>10000	>10000	>10000	>10000	>10000	>10000	>10000	>10000
(*S*)-**4n**	446(24)	5692(1120)	>10000	>10000	>10000	>10000	>10000	>10000
(*R*)-**4n**	480(80)	>10000	>10000	>10000	>10000	>10000	>10000	>10000
15	>10000	>10000	5750(1004)			>10000	919(133)	>10000
1	1584 (180)	794(99)	>10000					
5a [j]	138(14)	124(45)	>10000					
6a [k]	>10000	501(76)						
5-HT [k]	1.6(0.2)	1258(156)	100(8)					

[a] K_i in nM, derived from IC_{50} according to the method of Cheng and Prosoff. Values in parentheses are the mean ± SEM of three determinations. [b] [^{3}H]8-OHDPAT, rat hippocampus. [c] [^{3}H]ketanserin, rat cortex. [d] [^{3}H]GR113808, guinea pig striatum. [e] [^{3}H]prazosin, rat cortex. [f] [^{3}H]RX 821002, rat cortex. [g] [^{3}H]SCH-23390, rat striatum. [h] [^{3}H]spiperone, rat striatum. [i] [^{3}H]QNB, rat cortex. [j] From ref 12. [k] From ref 13.

Table 3. Agonist Potency in Guinea Pig Left and Right Atria and Aortic Strips and Antagonist Activity in Guinea Pig Right Atrium

	positive inotropy[a]		positive chronotropy[b]		contractility on aortic strips[c]		antagonist activity[d]
compd	pD$_2$ [e] ± SE	α[f]	pD$_2$ [e] ± SE	α[f]	pD$_2$ [e] ± SE	α [f]	pIC$_{50}$ [g] ± SE
5-HT	6.85 ± 0.12	1[h]	5.78 ± 0.09	1[h]	4.19 ± 0.09	1[h]	
PBG	4.31 ± 0.09	1[h]					
tropisetron	inactive[i]		inactive[i]		inactive[i]		7.52 ± 0.08[j]
2	5.51 ± 0.19	1[h]	5.06 ± 0.05	1[h]			
4a	inactive[i]		inactive[i]		inactive[i]		5.72 ± 0.13
4c	inactive[i]		inactive[i]		inactive[i]		4.95 ± 0.19
4h	inactive[i]		inactive[i]		inactive[i]		5.24 ± 0.14
4i	inactive[i]		inactive[i]		inactive[i]		5.07 ± 0.07
(*S*)-**4n**	inactive[i]		5.98 ± 0.10	0.81[k]	inactive[i]		
5a	inactive[i]		6.79 ± 0.09	0.60[k]	inactive[i]		

[a] Positive inotropic potency in guinea pig left atrium driver at 1 Hz. [b] Positive chronotropic potency in guinea pig spontaneously beating right atrium. Pretreatment ranged from 170 to 200 beats/min. [c] Positive contractility potency in guinea pig aortic strips. [d] Antagonist activity value in guinea pig spontaneously beating right atrium. The agonist was 5-HT. [e] $pD_2 = -\log EC_{50}$. EC_{50} values are calculated from log concentration−response curves (Probit analysis according to Litchfield and Wilcoxon[48]). pD_2 values are expressed as the mean ± SE of at least four independent experiments. [f] α = intrinsic activity of compound relative to 5-HT. [g] Each pIC_{50} value of noncompetitive antagonism was obtained from inhibition of compounds at three different concentrations. $pIC_{50} = -\log IC_{50}$. IC_{50} value, calculated from log concentration−response curves (Probit analysis according to Litchfield and Wilcoxon[48] with $n = 4-6$), is the concentration of the noncompetitive antagonist that inhibits 50% of maximum response to agonist. The values are expressed as the mean ± SE of five independent experiments performed. [h] Full agonist. [i] Inactive = no significant variation ($p < 0.05$) from the control at the maximum concentration tested (100 μM). [j] pA_2 ± SE values were calculated from Schild plots,[51] constrained to slope −1.0.[52] pA_2 is the positive value of the intercept of the line derived by plotting log(DR − 1) vs log [antagonist]. The log(DR − 1) was calculated from at least three different antagonist concentrations, and each concentration was tested from four to six times. Dose-ratio (DR) values represent the ratio of the potency of the agonist 5-HT (EC_{50}) in the presence of the antagonist and in its absence. Parallelism of concentration−curves was checked by linear regression, and the slope was tested for significance ($p < 0.05$). [k] Partial agonist.

Table 4. Functional Behavior of Compounds **4a**, **4c**, **4d**, **4h**, and **5a**

	von Bezold−Jarishreflex test	
compd	behavior	ID_{50},[a] μg/kg iv
4a	agonist	36 (ED_{50})
4c	antagonist	75
4d	antagonist	50
4h	partial agonist	30
5a [b]	antagonist	600

[a] The ID_{50} value is the test drug concentration that produces a 50% inhibition of the maximal effect induced by PBG. [b] From ref 12.

cyclic nitrogen), and (iii) an aromatic moiety (Table 1 of SI). Indeed the protonated nitrogen is involved in cation−π and/or charge assisted hydrogen bond, while different protein residues characterized by H-bond donor/acceptor groups assist the binding. The aromatic system of the ligand establishes π−π polarized interactions with several aromatic residues present along the receptor binding site (Figure 1 of SI).

Finally, on the basis of single pK_a values of the piperazine N-4 substituents (Table 1), compounds **4a**−**o** were grouped in two clusters: cluster A including compounds **4a**, **4b**, **4f**, **4k**, and **4m** (R′ single pK_a < 7), cluster B including compounds **4c**−**e**, **4g**−**i**, **4l**, (*S*)-**4n**, (*R*)-**4n**, and **4o** (R′ single pK_a > 7). Compounds in which R′ was characterized by more than one single pK_a value were clustered according to the resulting overall acidity, taking in to account R′ internal proton exchange. Compound **4j**, characterized by the presence of 100% anionic form at physiological pH (Table 1), was not included in this classification.

As revealed by the analysis of all conformers resulting from MM (data not shown) and AM1 geometry optimization (global minima reported in Table 2 of SI and Table 3 of SI) geometry optimization, our calculations resulted in coherent conformational trends. Geometrical parameters selected for organizing conformers into families were the following: (i) the distance between pyrroloquinoxaline N-1 and piperazine N-4 (d_1) and the height (h) of the piperazine N-4 with respect to the plane of the aromatic system, which are related to the conformation of the piperazine ring; (ii) the distance between the exchangeable hydrogen and the closest heteroatom ($d_{N4\text{-}X2}$, Table 2 of SI; $d_{N4\text{-}H\gamma/\delta}$, Table 3 of SI), demonstrating the presence (or not) of an intramolecular H-bond; (iii) the distances between the exchangeable hydrogen and the pyrroloquinoxaline system ($d_{N1\text{-}H4}$, $d_{X1\text{-}H4}$, Table 2 of SI; $d_{N1\text{-}H\gamma/\delta}$, $d_{X1\text{-}H\gamma/\delta}$, Table 3 of SI), indicative of piperazine rotation with respect to the pyrroloquinoxaline system. AM1 calculations resulted in two possible piperazine ring conformers: pseudoaxial chair ($h > 1.0$ Å) or pseudoequatorial chair ($h < 1.0$ Å). Piperazine ring pseudoaxial conformation was energetically favored in all compounds bearing a protonated piperazine N-4 (cluster A, Table 2 of SI), as well as for most of the structures belonging to cluster B (Table 3 of SI) with the exception of **4i** tautomer 2 and of all tautomers of **4l** and **4o**. MM indicated the sp^2 nature of the conjugated proximal nitrogen, thus with piperazine resulting in a pseu-

doequatorial position (Figure 2 of SI and Table 5 of SI). Taken together, these results suggested that the intramolecular attraction between exchangeable hydrogens and N-1 may affect piperazine conformation of **4a**−**o**. This was confirmed by the analysis of related distance values (i.e., $d_{N1\text{-}H4}$, cluster A; $d_{N1\text{-}H\gamma/\delta}$, cluster B). Interestingly, MM calculations simulating an aqueous environment ($\varepsilon = 80r$) and semiempirical AM1 calculations (performed in vacuum) revealed that the piperazine N-4 and R′ (Figure 2 of SI and Table 5 of SI) establish an intramolecular H-bond, in agreement with calculated pK_a values (Table 1).

Structure−**Activity Relationship Studies. Discussion.** Because of the nature of R′, the new derivatives **4a**−**o** presented piperazine N-4 single pK_a values 3−4 orders of magnitude lower than those of the reference compounds **1**, **5a**, **6a**, and **6b** (Table 1), in line with the reduced electron density at piperazine N-4 (e.g., AM1 ESP partial charge at piperazine N-4: **5a** (−0.10) vs **4a** (−0.02), Table 4 of SI). Accordingly, the calculated distribution of ionic species at physiological pH showed that most of the compounds are present in the neutral or in the zwitterionic form, depending on the single pK_a values of R′ and piperazine N-4 (Table 1). Despite the lack of a total net positive charge on the molecule (with the exception of **4o**) and the presence of acidic functional groups at piperazine N-4, compounds **4a**−**o** showed 5-HT$_3$R binding affinities from the low to the high nanomolar range (Table 1). The presence of a net negative charge on the molecule (which implies the lack of a key pharmacophoric element for 5-HT$_3$R ligands) is detrimental for 5-HT$_3$R affinity, **4j** being the least potent of the series (**4j**, 100% anionic at pH 7.2, $K_i = 246$ nM, Table 1).

Compounds belonging to cluster A (R′ single p$K_a < 7$, Table 1) are in equilibrium between their anionic and zwitterionic forms at pH 7.2 (Table 1 of the main text and Table 2 of SI). The almost identical single pK_a values of the amino and carboxyl functions of **4a** and **4b** (Table 1) allowed us to speculate about the presence of a rapid proton exchange equilibrium between the amino and the carboxyl groups. As demonstrated by the structural comparison depicted in Figure 3 of SI and by the distances reported in Table 2 of SI, either in the zwitterionic or in the neutral form, the exchangeable hydrogen is sufficiently close to the piperazine N-4 to fulfill the 5-HT$_3$R pharmacophore. Accordingly, although presenting a percentage of anionic form at pH 7.2 (Table 1), **4a** and **4b** showed low nanomolar 5-HT$_3$R affinity (**4a**, $K_i = 11.7$ nM; **4b**, $K_i = 2.1$ nM). The higher affinity of **4b** with respect to **4a** is due to the 7-OH substituent on the pyrroloquinoxaline ring system, which could (i) mimic the hydroxyl group of serotonin (Figure 1 of SI), thus acting as an additional H-bond donor/acceptor, or (ii) drive alternative binding modes of the anionic form of **4b**. Compounds (±)-**4f** and **4k**, although fulfilling 5-HT$_3$R pharmacophoric requirements when in the zwitterionic form (Table 2 of SI), are mostly present in the anionic form (Table 1), consequently showing lower 5-HT$_3$R affinity with respect to **4a** and **4b** (**4f**, $K_i = 44$ nM; **4k**, $K_i = 65$ nM). The extra volume occupied by the phenyl substituent of (±)-**4f** could play a role in receptor affinity (see discussion below; Figure 4 of SI). In the case of **4m**, only the tautomer 1 was calculated to be mostly (55%) present in the zwitterionic form while 100% of tautomer 2 was anionic at physiological pH (Table 1). Moreover, despite what occurred for **4a**, **4b**, **4f**, and **4k**, tautomer 1 of **4m** is not stabilized by an intramolecular H-bond with piperazine N-4 ($d_{H4\text{-}X2}$, Table 2 of SI). Accordingly, **4m** was the least potent compound of cluster A toward 5-HT$_3$R (**4m**, $K_i = 127$ nM). In summary, 5-HT$_3$R affinity of cluster A mainly correlates with the calculated percentage of anionic form at physiological pH and with the availability of an exchangeable hydrogen in the molecule. These SARs indicated that to obtain compounds with decreased BBB permeability and still endowed with high 5-HT$_3$R affinity, a crucial issue is the "masking" of the acidic function R′ (Table 1) through an internal proton exchange with the basic distal piperazine nitrogen.

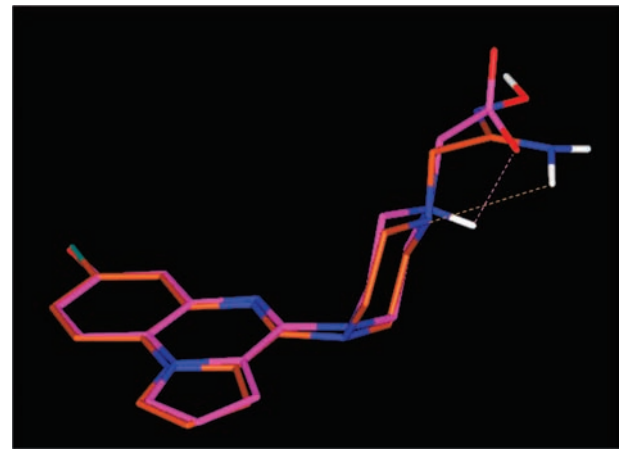

Figure 1. Superimposition (aromatic heavy atoms and exchangeable hydrogen) of the AM1 global minimum conformers of **4b** (magenta carbon atoms) and of **4h** tautomer 1 (orange carbon atoms). Nitrogen atoms are in blue and oxygen atoms in red. Only exchangeable hydrogens are shown, for the sake of clarity. H-bonds are highlighted with dashed lines and colored as carbon atoms.

Compounds of cluster B (**4c**−**e**, **4g**−**i**, **4l**, (*S*)-**4n**, (*R*)-**4n**, and **4o**, Table 1) bearing "mild" acidic piperazine N-4 substituents (p$K_a > 7$) do not present an anionic form at physiological pH, with the exception of **4l**, and most of them present the neutral form as the most abundant one. Therefore, their bioactive form presents piperazine N-4 always deprotonated with the exchangeable hydrogen located on the R′ substituent heteroatom at the γ or δ position with respect to piperazine N-4 (Table 1 of the main text, Table 3 of SI, and Figure 1).

Compounds **4d**, **4e**, **4h**, (*S*)-**4n**, (*R*)-**4n**, and **4i** displayed 5-HT$_3$R affinity in the range of 0.8 and 3.4 nM, **4h** being as potent as the reference compound **5a** (Table 1). Accordingly, they share the hypothesized key pharmacophoric features, namely, the presence in tautomer 1 of a polarized H-bond between R′(H$_\gamma$) and piperazine N-4 ($d_{N4\text{-}H\gamma/\delta}$ in Table 3 of SI) and they show the same distances between the exchangeable hydrogen and the other pharmacophoric groups, i.e., N-1 and the pyrroloquinoxaline system ($d_{N1\text{-}H\gamma/\delta} \approx 6.6$ Å and $d_{X1\text{-}H\gamma/\delta} \approx 8.6$ Å, Table 3 of SI; **4h** tautomer 1 vs **4b**, Figure 1). **4h**, the most active compound of the whole series, also presents tautomer 2 stabilized by an internal H-bond with R′(H$_\delta$), together with the correct orientation of the pharmacophoric groups ($d_{N1\text{-}H\gamma/\delta} = 6.5$ Å and $d_{X1\text{-}H\gamma/\delta} = 8.5$ Å, Table 3 of SI). Compound **4c** also shows nanomolar affinity ($K_i = 7.3$ nM, Table 1), although being slightly less potent than the above-mentioned set of compounds. Affinity data of **4c**, presenting an amide moiety, confirmed a correlation between the 5-HT$_3$R affinity and the acidity of the exchangeable hydrogen (i.e., single pK_a value, Table 1). Furthermore, taking into account **4n**, the similar 5-HT$_3$R affinity shown by the two enantiomers (Table 1) indicates a receptor tolerance in accommodating a carboxyl function close to piperazine N-4 (Figure 2), in agreement with what was observed for **4b** and **4h** (Figures 1 and 2). Apart from **4h**, **4l** is the only compound presenting a second tautomer with an internal H-bond between R′(H$_\gamma$) and piperazine N-4 ($d_{N4\text{-}H\gamma/\delta}$, Table 3 of SI).

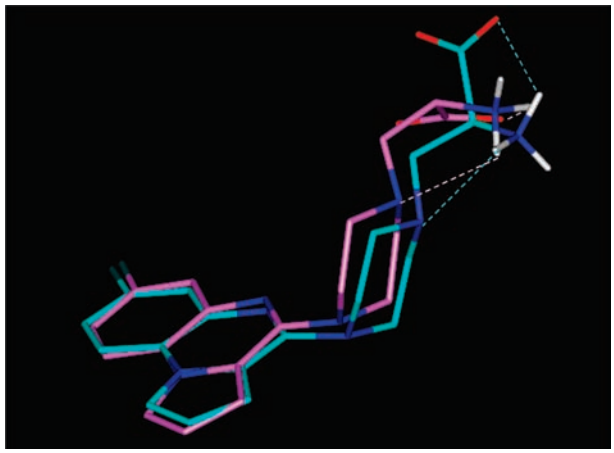

Figure 2. Superimposition (aromatic heavy atoms and exchangeable hydrogen) of the AM1 global minimum conformer of (*R*)-**4n** (pink carbon atoms) and a low energy conformer of (*S*)-**4n** (cyan carbon atoms) ($\Delta E_{AM1} = 0.6$ kcal/mol). Nitrogen atoms are in blue and oxygen atoms in red. Only exchangeable hydrogens are shown, for the sake of clarity. H-bonds are highlighted with dashed lines and colored as carbon atoms.

Nevertheless, its 5-HT$_3$R affinity is lower than that of **4h** (**4h** $K_i = 0.8$ nM vs **4l** $K_i = 17$ nM, Table 1). This can be explained considering that **4l**, because of the presence of the carbonyl oxygen on the triazole ring, presents four tautomeric forms. The availability of an exchangeable hydrogen close to piperazine N-4 is not preserved in all tautomers as it occurs for **4h** (Table 3 of SI). Furthermore, two out of four **4l** tautomers show a calculated percentage of the anionic form at physiological pH (Table 1), in agreement with its reduced affinity with respect to **4h**. Compounds (±)-**4g** ($K_i = 79$ nM) and (±)-**4f** ($K_i = 44$ nM), characterized by a bulky phenyl substituent at piperazine N-4, show a nearly comparable affinity, even though (±)-**4f** was predicted to be mostly present in the anionic form and (±)-**4g** in the neutral one (Table 1). The activity of (±)-**4g** compared to that of (±)-**4f** could be ascribed (i) to the different location of the volume occupied by the phenyl group caused by intramolecular H-bond formation (Figure 4 of SI), and/or (ii) to the higher acidity of the hydrogen-donor group of (±)-**4f** with respect to the alcoholic group of (±)-**4g** (i.e., single pK_a values, Table 1). The serine derivative **4o** was much less potent ($K_i = 237$ nM), although being the only compound of the whole series predicted to be mostly (94%) present in the protonated form at pH 7.2. The lower 5-HT$_3$R affinity of **4o** (**4o** vs **4n**) is in full agreement with the SARs emerging from our analysis. As a result of the reduced availability of the nitrogen lone pair (N-4) and of the reduced flexibility of the carbonyl group, **4o** does not present an H-bond with R′ ($d_{N4\text{-}H\gamma/\gamma\delta/\delta} = 3.8$, 3.2 Å, Table 3 of SI) (**4o** vs **4n**, Figure 3). By consequence, **4o** does not present the correct orientation of the exchangeable hydrogen with respect to the other pharmacophoric groups ($d_{N1\text{-}H\gamma/\delta} = 8.3$, 4.0 Å; $d_{X1\text{-}H\gamma/\delta} = 10.4$, 7.0 Å).

In conclusion, the presence of a net positive charge on the molecule and the protonation at piperazine N-4 are not necessary for high 5-HT$_3$R affinity (e.g., **4h** vs **5a**, Table 1). A net negative charge on the molecule is detrimental for the affinity (**4j**), while the presence of an exchangeable hydrogen close to piperazine N-4 is required. Indeed, the formation of an intramolecular H-bond between piperazine N-4 and the hydrogen at R′ is related to high affinity likely because it results in a correct orientation of the exchangeable pharmacophoric hydrogen. Furthermore, a correlation between exchangeable hydrogen acidity and 5-HT$_3$R affinity was found, thus suggesting that polarization plays a role in interaction with the receptor. On these bases, it can be stated that, at least in our series of derivatives, the cation−π and/or salt-bridge interaction proposed for the amine nitrogen in different receptor interaction models can be replaced with a polarized H-bond interaction to obtain equally active compounds with decreased BBB permeability.

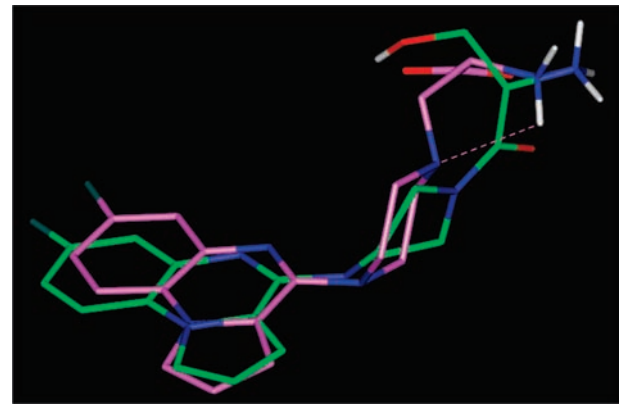

Figure 3. Superimposition on pharmacophoric points (aromatic heavy atoms, including the aryl nitrogen, and exchangeable hydrogen) of the AM1 global minimum conformers of (*R*)-**4n** (pink carbon atoms) and **4o** (green carbon atoms). Nitrogen atoms are in blue and oxygen atoms in red. Only exchangeable hydrogens are shown, for the sake of clarity. H-bonds are highlighted with dashed lines and colored as carbon atoms.

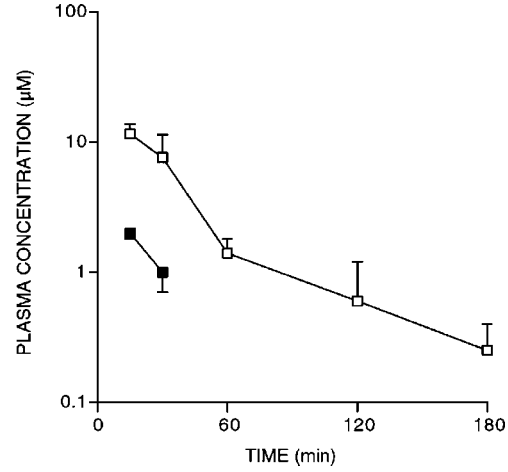

Figure 4. Mean plasma concentration−time curves of compound (*S*)-**4n** after ip injection in the mouse. Each value is the mean ± SD of three mice for the 5 (closed symbol) and 20 mg/kg doses (open symbol). Compound (*S*)-**4n** was generally undetectable in the brain, but in one animal each, 15 and 30 min after dosing, it reached levels close to the limit of quantitation of the method (about 0.5 nmol/g).

Functional in Vitro Assays. Assessment of Cardiovascular Activity of 4a, 4c, 4h, 4i, (*S*)-4n, and 5a on Isolated Atria under the Effect of 5-HT. 5-HT induces a positive chronotropic and inotropic effect in isolated right and left atria preparations, respectively. This effect is mimicked by 5-HT$_3$R agonists such as **2**, 1-phenylbiguanide (PBG), and **1** (a brain-penetrating compound).[10] We therefore evaluated the effects produced by a subset of compounds on isolated atrial preparation after treatment with 5-HT. Modulation of cardiovascular parameters by compounds **4a**, **4c**, **4h**, **4i**, (*S*)-**4n**, **5a**, and reference 5-HT$_3$R ligands is reported in Table 3. All tested compounds are devoid of positive inotropic activity and do not induce vasoconstriction. While compounds **4a**, **4c**, **4h**, and **4i**

show antagonist activity, (*S*)-**4n** potently modulates chronotropy, as well as 5-HT. In particular **4a**, **4c**, **4h**, and **4i** were noncompetitive antagonists of the effect induced by 5-HT on cardiac 5-HT_3R (pIC_{50} = 5.72, 4.95, 5.24, and 5.07, respectively, Table 3), while tropisetron was found to be a competitive antagonist of 5-HT_3R (pA_2 = 7.52). Compound (*S*)-**4n** was a partial agonist (α = 0.81) 1.6- and 8.3-fold more potent than 5-HT and **2**, respectively (pD_2 = 5.98, 5.78, and 5.06, respectively, Table 3). These results indicate that (*S*)-**4n** specifically acts at the right atrium through 5-HT_3Rs. Moreover, compound **5a** showed a weak partial agonist activity (α = 0.60) at the right atrium level. Finally the peculiar cardiac activity of (*S*)-**4n** and **5a**, eliciting an effect only at the right atrium level, might be due to selective action on a subpopulation of 5-HT_3Rs. Further investigations are needed in order to assess this important issue.

Functional in Vivo Assays. von Bezold−Jarish Reflex Test. In vivo investigations on the 5-HT_3R-dependent von B-J reflex in urethane-anesthetized rats (1.6 g/kg intraperitoneal (ip))[38] (Table 4) supported a different behavior for the tested quinoxalines, with respect to that observed in the in vitro assays performed on isolated atria preparation. The results ranged from the agonist properties of **4a** and the partial agonist properties of **4h** to the antagonist properties of **4c**,**d**, and **5a**. The von B-J reflex is a cardiovascular reflex that has been demonstrated to involve the activation of central 5-HT receptors. However, it could also be mediated by stimulation of 5-HT_3Rs located in the cardiopulmonary area, in particular on sensory vagal nerve endings in the heart, atrium, and ventricles. Substances experimentally used to elicit the von B-J reflex include veratridine, 5-HT, and PBG, a selective 5-HT_3R agonist. PBG caused dose-dependent fall of heart rate and arterial pressure when injected into the left or right atrium of unanesthetized animals. PBG acts as an agonist through pharmacologically specific 5-HT_3Rs. So, PBG (agonist) and zacopride (antagonist) were tested as reference 5-HT_3R ligands on von B-J reflex. PBG (40 μg/kg, iv) produced a marked transient bradycardia (64% decrease in heart rate within the first 30 s after injection). Its effects are prevented by pretreatment with zacopride (1 μg/kg, iv, 5 min before PBG administration). Therefore, each tested compound was injected iv 5, 15, 30 min prior PBG to assess their potential antagonist effect.

When compound **4a**, an agonist at 5-HT_3Rs, was administered alone, it mediated the von B-J reflex with an efficacy close to that of PBG (ED_{50} value of 36 μg/kg (iv)), producing a transient bradycardia similar to that observed after the iv injection of 40 μg/kg of PBG. At the same dose, **4a** only exerted marginal effects on the bradycardia evoked by PBG, indicating negligible antagonist properties at cardiac 5-HT_3Rs.

Compound **4c** dose-dependently inhibited PBG-induced bradycardia with an ID_{50} value of 75 μg/kg (iv). This pyrroloquinoxaline was unable, at 50 μg/kg (iv), to affect heart rate in urethane-anesthetized rats. However, pretreatment with 50 μg/kg (iv) of **4c** significantly attenuated the bradycardia elicited by subsequent injection of PBG (40 μg/kg, iv). The effect persisted to the same extent (−35% to −45%) for at least 30 min after administration of **4c**. These data led to the conclusion that **4c** is an antagonist at cardiac 5-HT_3Rs, even though its potency is lower than that of zacopride (100% prevention at 1 μg/kg, iv). The hydroxamic acid derivative **4d**, a potent 5-HT_3R ligand, also exerted a dose-dependent antagonist action, since it could prevent PBG-induced bradycardia, with an ID_{50} value of 50 μg/kg (iv). We also characterized **5a** at the cardiac level.[13] Compound **5a** was used as a reference drug because it binds 5-HT_3R with high affinity and is brain-permeable. In this test, with an ID_{50} of 600 μg/kg (iv), compound **5a** exerted antagonist activity, even though it is less potent than **4c** and **4d**.

The partial agonist **4h**, at a dose of 50 μg/kg (iv), induced a transient bradycardia that was about 60% of that due to PBG (40 μg/kg, iv). In addition to this agonist effect, **4h** also exerted an antagonist action, since it can prevent PBG-induced bradycardia. In this case the effect of **4h** was clearly dose-dependent, with half-blockade at 30 μg/kg when this drug was injected 5 min before PBG. The behavior of (*S*)-**4n** was difficult to interpret. In fact after iv injection at a dose of 100 μg/kg, in contrast to PBG, (*S*)-**4n** on its own did not alter heart rate. A significant reduction in PBG-evoked bradycardia was found by pretreating the rats with (*S*)-**4n**, but the effect was not time-dependent and not reproducible in all rats (2 out of 7).

Brain-to-Plasma Distribution Studies. Mice were given compound (*S*)-**4n** ip and were sacrificed at various times thereafter for obtaining basic information on the concentrations achieved in brain after doses of potential pharmacological interest and for obtaining their relationship with plasma concentrations. Figure 4 shows the mean plasma concentration−time curves of (*S*)-**4n** after 5 and 20 mg/kg. The compound rapidly reached the systemic circulation with maximal plasma concentrations (2 and 12 μM at 5 and 20 mg/kg, respectively) already 15 min after dosing (i.e., the first sampling time). At the lower dose the assay was not sensitive enough for following plasma concentrations for more than 30 min. This rapid decay probably approximates the distribution phase of the compound. In fact, a parallel distribution phase was also observed at 20 mg/kg, but this was followed by a slower decay, between 30 and 180 min after dosing. The elimination half-life (0.693/β) associated with this phase averaged 53 min, this being the result of the high clearance in conjunction with a relatively high volume of distribution of this compound (Cl = dose *F*/AUC = 90 (mL/min)/kg; Vd/*F* = C1/β = 6 L/kg, assuming complete absorption of (*S*)-**4n** from the ip site). This pharmacokinetic behavior is consistent with that of other pyrroloquinoxalines and structurally related compounds such as arylpiperazines and their derivatives.[12,13,39]

In previous work, we evaluated the ability of pyrroloquinoxaline and arylpiperazine derivatives to cross the BBB in vivo in rodents. Most of them rapidly entered the rat brain, achieving whole brain concentrations higher than in plasma, although with differences in the brain-to-plasma partition value.[12,13,39] This is explained by their lipophilicity, which allows free and rapid diffusion across the BBB.[40] An exception was a pyrroloquinoxaline derivative with a hydrophilic (carboxylic) group at the piperazine ring (compound **7b** as the internal standard (IS) of the present HPLC procedure) for which the brain-to-plasma distribution ratio averaged only 0.1 after 5 mg/kg in rats.[13]

Compound (*S*)-**4n** was generally undetectable in mouse brain after ip doses, suggesting poor BBB permeability. However, after 20 mg/kg it reached brain concentrations close to the limits of quantitation of the analytical procedure (about 0.5 μM assuming 1 g of tissue equivalent to 1 mL of water) in only two animals (n = 2) within 15−30 min of dosing. In these cases, plasma concentrations averaged 10 μM.

Preliminary brain-to-plasma distribution studies were also performed for compound **4a**. Analogously to compound **7b**,[13] **4a** mean plasma concentrations exceeded those in brain.

Conclusions

This work led to the discovery of potent and selective 5-HT_3R ligands with poor BBB permeability due to their unique structural features. The intrinsic pharmacological properties and

the cardiac modulatory activity of the new compounds was assessed by means of in vitro (functional preparations) and in vivo (von B-J reflex test) studies. Because the compounds were based on a pyrroloquinoxaline skeleton, the unique pharmacological properties of the novel modulators are mainly due to the key substituents at the piperazine N-4. In cardiac tissue, while 5-HT and **2** stimulate inotropic and chronotropic activity (isolated left and right atria 5-HT$_3$R) and 5-HT, but not **2**, induces vasoconstriction (non-5-HT$_3$R), several of the new compounds herein reported showed antagonism or partial agonism of the positive chronotropy (right atrium) induced by 5-HT without affecting inotropy (left atrium). Among these compounds **4c**, **4h**, and **4i** were shown to be potent antagonists in functional assays, selective for those 5-HT$_3$Rs localized in guinea pig right atrium (no vasoconstriction). Compound (*S*)-**4n** was found as a potent cardiomodulator of the chronotropy parameter with no effects on inotropy, indicating a selective action on 5-HT$_3$Rs localized at the right atrium. These compounds may pave the way for the future development of new peripherally acting 5-HT$_3$R subtype-selective cardiomodulators. In vivo functional evaluation (von B-J reflex) of a subset of compounds was substantially in line with their in vitro functional evaluation with the exception of compounds **4a**, characterized by a zwitterionic substituent at the piperazine N-4, which was an agonist.

In summary, the design of selective 5-HT$_3$R ligands poorly penetrating the brain represents a valuable strategy to develop novel cardiomodulators with minimized central side effects, being an important step in the progression toward peripherally acting 5-HT$_3$R ligands for the treatment of a variety of diseases. Compounds **4a** and **4n** represent novel pharmacological tools to investigate the role of putative 5-HT$_3$R subpopulations at the cardiac level.

Experimental Section

Reagents were purchased from Sigma-Aldrich and were used as received. Reaction progress was monitored by TLC using Merck silica gel 60 F_{254} (0.040−0.063 mm) with detection by UV. Merck silica gel 60 (0.040−0.063 mm) was used for flash chromatography. Melting points were determined using an Electrothermal 8103 apparatus. IR spectra were taken with Perkin-Elmer 398 and FT 1600 spectrophotometers. ^{1}H NMR spectra were recorded on a Brüker 200 spectrometer with TMS as internal standard. Splitting patterns are described as singlet (s), doublet (d), triplet (t), quartet (q), and broad (br). The value of chemical shifts (δ) are given in ppm and coupling constants (*J*) in hertz (Hz). All reactions were carried out in an argon atmosphere. Elemental analyses were performed on a Perkin-Elmer 240 °C elemental analyzer, and the results were within ±0.4% of the theoretical values (purity >95%). Yields refer to purified products and are not optimized.

[4-(7-Fluoropyrrolo[1,2-*a*]quinoxalin-4-yl)piperazin-1-yl]acetic Acid Ethyl Ester (11a). Diisopropylethylamine (DIPEA) (85.0 mg, 0.66 mmol) and ethyl bromoacetate (0.120 g, 0.75 mmol) were added to a solution of **10a** (0.120 g, 0.44 mmol) in acetonitrile (10 mL). The mixture was stirred at room temperature for 12 h. The solvent was evaporated, and the residue was dissolved in dichloromethane (DCM) and washed with water (10 mL). The organic phase was dried over sodium sulfate and evaporated. The residue was purified by flash chromatography (1:1 *n*-hexane/ethyl acetate) to give **11a** (0.140 g, 89%) as colorless prisms (mp 208−210 °C, *n*-hexane). ^{1}H NMR ($CDCl_3$) δ 1.28 (t, 3H, J = 6.9 Hz), 2.79 (m, 4H), 3.31 (s, 2H), 3.91 (m, 4H), 4.22 (m, 2H), 6.78 (q, 2H, J = 6.9 Hz), 6.92 (m, 1H), 7.33 (m, 1H), 7.65 (m, 1H), 7.78 (m, 1H); IR (chloroform) 1728 cm^{-1}.

[4-(9-Methylpyrrolo[1,2-*a*]quinoxalin-4-yl)piperazin-1-yl]acetic Acid Ethyl Ester (11b). From **10b** and ethyl bromoacetate, the title compound was obtained in 88% yield following the procedure described for **11a**. After recrystallization **11b** was obtained as yellow prisms (mp 217−221 °C, *n*-hexane). ^{1}H NMR ($CDCl_3$) δ 1.28 (t, 3H, J = 7.0 Hz), 2.80 (m, 4H), 2.86 (s, 3H), 3.30 (s, 2H), 3.83 (m, 4H), 4.22 (q, 2H, J = 7.0 Hz), 6.75 (m, 2H), 7.07 (m, 1H), 7.21 (m, 1H), 7.57 (m, 1H), 8.13 (m, 1H); IR (chloroform) 1732 cm^{-1}.

[4-(7-Fluoropyrrolo[1,2-*a*]quinoxalin-4-yl)piperazin-1-yl]acetic Acid Benzyl Ester (11c). A suspension of **10a** (0.200 g, 0.74 mmol), anhydrous potassium carbonate (0.960 g, 0.74 mmol), and benzyl bromoacetate (0.170 g, 0.74 mmol) in 2-butanone (33 mL) was heated under reflux for 1 h under argon atmosphere. The solvent was evaporated, and the residue was partitioned between water (15 mL) and DCM (30 mL). The organic layer was washed with brine, dried over sodium sulfate, and evaporated. The residue was purified by flash chromatography (1:5 DCM/ethyl acetate) to give **11c** (0.220 g, 72%) as colorless prisms (mp 165−167 °C, ethyl acetate). ^{1}H NMR ($CDCl_3$) δ 2.79 (m, 4H), 3.36 (s, 2H), 3.90 (m, 4H), 5.19 (s, 2H), 6.76 (m, 2H), 6.97 (m, 1H), 7.36 (m, 6H), 7.65 (m, 1H), 7.75 (m, 1H); IR (Nujol) 1681, 1622 cm^{-1}.

[4-(7-Benzyloxypyrrolo[1,2-*a*]quinoxalin-4-yl)piperazin-1-yl]acetic Acid Benzyl Ester (11d). From **10c**, the title compound was obtained in 77% yield following the procedure described for **11c**. After recrystallization, **11d** was obtained as pale-yellow prisms (mp 115−118 °C, ethyl acetate). ^{1}H NMR ($CDCl_3$) δ 2.60 (m, 4H), 3.37 (s, 2H), 3.82 (m, 4H), 5.15 (s, 2H), 5.19 (s, 2H) 6.73 (m, 2H), 6.96 (m, 1H), 7.22−7.48 (m, 11H), 7.63 (m, 1H), 7.72 (m, 1H); IR (Nujol) 1675, 1628 cm^{-1}.

7-Fluoro-4-(4-cyanomethylpiperazin-1-yl)pyrrolo[1,2-*a*]quinoxaline (12). A mixture of **10a** (0.220 g, 0.83 mmol), anhydrous potassium carbonate (0.110 g, 0.83 mmol), and bromoacetonitrile (58 μL, 0.83 mmol) in 2-butanone (35 mL) was heated under reflux for 3 h under argon atmosphere. The solvent was evaporated, and the residue was partitioned between water (15 mL) and DCM (30 mL). The organic layer was washed with brine, dried over sodium sulfate, and concentrated. The residue was purified by flash chromatography (1:3 DCM/ethyl acetate) to give **12** (0.187 g, 73%) as colorless prisms after recrystallization (mp 147−149 °C, 1:1 ethyl acetate/*n*-hexane). ^{1}H NMR ($CDCl_3$) δ 2.80 (m, 4H), 3.61 (s, 2H), 3.86 (m, 4H), 6.76 (m, 2H), 6.97 (m, 1H), 7.33 (m, 1H), 7.65 (m, 1H), 7.76 (m, 1H); IR (Nujol) 2245 cm^{-1}.

[4-(7-Fluoropyrrolo[1,2-*a*]quinoxalin-4-yl)piperazin-1-yl]acetic Acid (4a). A solution of **11c** (0.230 g, 0.55 mmol) in methanol (5 mL) was hydrogenated at atmospheric pressure over 10% Pd/C for 1 h. The catalyst was removed by filtration over Celite, the filtrate was evaporated, and the residue was recrystallized from ethyl acetate to provide **4a** (0.161 g, 89%) as colorless prisms (mp 219−221 °C, *n*-hexane). ^{1}H NMR (DMSO-d_6) δ 2.72 (m, 4H), 3.25 (s, 2H), 3.81 (m, 4H), 6.78 (m, 1H), 6.94 (m, 1H), 7.15 (m, 2H), 8.12 (m, 1H), 8.31 (m, 1H), 11.05 (br, 1H); IR (Nujol) 1715 cm^{-1}. Anal. ($C_{17}H_{17}N_4O_2F$) C, H, N.

[4-(7-Hydroxypyrrolo[1,2-*a*]quinoxalin-4-yl)piperazin-1-yl]acetic Acid (4b). From **11d**, the title compound was treated with 10% Pd/C for 12 h and was obtained as described for the preparation of **4a** in 85% yield. After recrystallization, **4b** was obtained as colorless prisms (mp 140−141 °C, *n*-hexane). ^{1}H NMR (DMSO-d_6) δ 2.69 (m, 4H), 3.12 (s, 2H), 3.68 (m, 4H), 6.69 (m, 2H), 6.85 (m, 2H), 7.86 (m, 1H), 8.15 (m, 1H); IR (Nujol) 1705 cm^{-1}. Anal. ($C_{17}H_{18}N_4O_3$) C, H, N.

2-[4-(7-Fluoropyrrolo[1,2-*a*]quinoxalin-4-yl)-piperazin-1-yl]acetamide (4c). Finely powdered potassium hydroxide (0.130 g, 2.3 mmol) was added to a stirred solution of **12** (0.200 g, 0.65 mmol) in *tert*-butyl alcohol (5 mL). The reaction mixture was heated under reflux for 35 min with vigorous stirring. The mixture was cooled to room temperature and poured into an aqueous sodium chloride solution, and the aqueous phase was extracted with chloroform (3 × 30 mL). The organic layers were dried over sodium sulfate and concentrated in vacuo. The crude product was purified by flash chromatography (1:3 ethyl acetate/chloroform). After recrystallization **4c** (0.150 g, 71%) was obtained as a yellow solid (mp 148−150 °C, *n*-hexane). ^{1}H NMR (CD_3OD) δ 2.62 (m, 4H), 2.98 (s, 2H), 3.81 (m, 4H), 6.82 (m,

1H), 6.96 (m, 1H), 7.12 (m, 2H), 7.29 (m, 2H); IR (Nujol) 1655 cm^{-1}. Anal. ($C_{17}H_{18}N_5OF$) C, H, N.

[4-(7-Fluoropyrrolo[1,2-*a*]quinoxalin-4-yl)piperazin-1-yl]hydroxyacetamide (4d). A solution of potassium hydroxide (0.180 g, 3.21 mmol) in methanol (0.86 mL) was added to a solution of hydroxylamine hydrochloride (0.130 g, 2.0 mmol) in methanol (0.80 mL). The resulting suspension was stirred at 0 °C for 1 h. Afterward it was filtered into a solution of compound **11a** (0.100 g, 0.28 mmol) in methanol (0.53 mL). The reaction mixture was stirred at room temperature for 15 min and concentrated to dryness. The residue was dissolved in water (1.1 mL), and the aqueous phase was acidified to pH 5 with 1 N hydrochloric acid and extracted with ethyl acetate (3 × 20 mL). The organic layer was washed with water, dried over sodium sulfate, and evaporated. The crude product was purified by flash chromatography (ethyl acetate) to give, after recrystallization, **4d** (56 mg, 59%) as colorless prisms (mp 159−160 °C, 1:1 ethyl acetate/*n*-hexane). ^{1}H NMR (CD_3OD) δ 2.66 (m, 4H), 3.21 (s, 2H), 3.78 (m, 4H), 6.68 (m, 1H), 6.81 (m, 1H), 6.93 (m, 1H), 7.19 (m, 1H), 7.81 (m, 1H), 7.93 (m,1H); IR (Nujol) 1668, 1635, 1468, 1443 cm^{-1}. Anal. ($C_{17}H_{18}N_5O_2F$) C, H, N.

[4-(9-Methylpyrrolo[1,2-*a*]quinoxalin-4-yl)piperazin-1-yl]hydroxyacetamide (4e). From **11b**, the title compound was prepared in 62% yield following the procedure described for **4d**. After recrystallization, **4e** was obtained as a yellow prisms (mp 165−166 °C, 1:1 ethyl acetate/*n*-hexane). ^{1}H NMR (DMSO-d_6) δ 2.62 (m, 4H), 2.82 (s, 3H), 2.95 (s, 2H), 3.65 (m, 4H), 6.79 (m, 1H), 6.90 (m, 1H), 7.12 (m, 1H), 7.21 (m, 1H), 7.42 (m, 1H), 8.25 (m, 1H), 8.80 (br, 1H), 10.49 (br, 1H); IR (Nujol) 1659, 1639, 1471, 1447 cm^{-1}. Anal. ($C_{18}H_{21}N_5O_2$) C, H, N.

[4-(9-Methylpyrrolo[1,2-*a*]quinoxalin-4-yl)piperazin-1-yl]phenylacetic Acid (4f). From **10b** and 1-bromophenylacetic acid ethyl ester, [4-(9-methylpyrrolo[1,2-*a*]quinoxalin-4-yl)piperazin-1-yl]phenyl acetic acid ethyl ester was prepared in 80% yield following the procedure described for **11a** and, after recrystallization, was obtained as yellow prisms (mp 209−211 °C, *n*-hexane). ^{1}H NMR ($CDCl_3$) δ 1.30 (t, 3H, J = 7.0 Hz), 2.59 (m, 2H), 2.63 (m, 2H), 2.82 (s, 3H), 3.59 (m, 4H), 3.88 (m, 1H), 4.25 (q, 2H, J = 7.0 Hz), 6.78 (m, 1H), 6.82 (m, 1H), 7.00−7.42 (m, 6H), 7.49 (m, 2H), 8.24 (m, 1H). The above compound (0.150 g, 0.35 mmol) was dissolved in tetrahydrofuran (THF, 2.8 mL), and while the mixture was being stirred, a solution of lithium hydroxide (25.0 mg, 1.0 mmol) in water (1.9 mL) was added dropwise. The reaction mixture was heated under reflux for 3 h. After this time, THF was removed under reduced pressure and the residue was treated with water, acidified, and extracted with ethyl acetate (3 × 10 mL). The organic phase was dried over sodium sulfate and evaporated. The residue was purified by flash chromatography (3:1 ethyl acetate/methanol) to give, after recrystallization, **4f** (0.133 g, 89%) as pale-yellow prisms (mp 225 °C dec, *n*-hexane). ^{1}H NMR (DMSO-d_6) δ 2.53 (m, 2H), 2.66 (m, 2H), 2.80 (s, 3H), 3.63 (m, 4H), 3.85 (m, 1H), 6.74 (m, 1H), 6.86 (m, 1H), 7.09−7.37 (m, 6H), 7.46 (m, 2H), 8.22 (m, 1H), 10.09 (br, 1H); IR (Nujol) 1733 cm^{-1}. Anal. ($C_{24}H_{24}N_4O_2$) C, H, N.

2-[4-(9-Methylpyrrolo[1,2-*a*]quinoxalin-4-yl)piperazin-1-yl]-2-phenylethanol (4g). Lithium borohydride (2.0 M solution in THF, 460 μL, 0.94 mmol) was added dropwise to a solution of [4-(9-methylpyrrolo[1,2-*a*]quinoxalin-4-yl)piperazin-1-yl]phenyl acetic acid ethyl ester (0.100 g, 0.23 mmol) in dry THF (2.5 mL). The reaction mixture was heated under reflux for 12 h and quenched with methanol and 1 N hydrochloric acid. Evaporation of reaction mixture gave a yellow oil which was treated with water and extracted with ethyl acetate. The organic phase was dried over sodium sulfate and evaporated to give an oil which was purified by flash chromatography (20:1 ethyl acetate/methanol). Compound **4g** (70.0 mg, 79%) was obtained, after recrystallization, as yellow prisms (mp 122−123 °C, *n*-hexane). ^{1}H NMR ($CDCl_3$) δ 2.58 (m, 2H), 2.82 (m, 6H), 3.76 (m, 6H), 4.05 (m, 1H), 6.69 (m, 2H), 7.08 (m, 1H), 7.23 (m, 3H), 7.34 (m, 3H), 7.53 (m, 1H), 8.11 (m, 1H); IR (chloroform): 1063 cm^{-1}. Anal. ($C_{24}H_{26}N_4O$) C, H, N.

[4-(7-Fluoropyrrolo[1,2-*a*]quinoxalin-4-yl)piperazin-1-yl]hydroxyacetamidine (4h). Compound **12** (0.100 g, 0.32 mmol), hydroxylamine hydrochloride (44.0 mg, 0.64 mmol), and sodium carbonate (67.0 mg, 0.64 mmol) were dissolved in ethanol (6.5 mL) and heated under reflux for 24 h. After filtration of inorganic salts, the solvent was evaporated under reduced pressure. The product was purified by flash chromatography (9:1 DCM/methanol) to provide, after recrystallization, **4h** (68.0 mg, 55%) as colorless prisms (mp 155−157 °C, *n*-hexane). ^{1}H NMR (DMSO-d_6) δ 2.51 (s, 2H), 3.10 (m, 4H), 3.78 (m, 4H), 5.30 (br, 2H), 6.70−7.30 (m, 5H), 8.10 (m,1H), 9.00 (br, 1H); IR (Nujol) 3225, 765 cm^{-1}. Anal. ($C_{17}H_{19}N_6OF$) C, H, N.

7-Fluoro-4-[4-(4*H*-[1,2,4]triazol-3-ylmethyl)-piperazin-1-yl]pyrrolo[1,2-*a*]quinoxaline (4i). A mixture of **10a** (0.200 g, 0.93 mmol), anhydrous potassium carbonate (0.250 g, 1.86 mmol), and *N*-formyl-2-chloroacetamidohydrazone[17] (0.188 g, 1.39 mmol) in anhydrous *N*,*N*-dimethylformamide (*N*,*N*-DMF, 8 mL) was heated to 60 °C for 3 h and to 130 °C for the next 12 h. The reaction mixture was cooled to room temperature and diluted with ethyl acetate. The organic layer was washed with water, dried over sodium sulfate, and evaporated. The resulting brown oil was purified by flash chromatography (7:3 ethyl acetate/petroleum ether) to afford, after recrystallization, **4i** (0.530 g, 81%) as colorless prisms (mp 209−210 °C, ethyl acetate). ^{1}H NMR (CD_3OD) δ 3.28 (m, 4H), 4.25 (m, 4H), 4.37 (s, 2H), 6.81 (m, 2H), 7.18 (m, 1H), 7.46 (m, 1H), 7.76 (m, 1H), 7.81 (m, 1H), 8.22 (m, 1H); IR (Nujol) 1679 cm^{-1}. Anal. ($C_{18}H_{18}N_7F$) C, H, N.

7-Fluoro-4-[4-(methanesulfonamidoacetyl)piperazin-1-yl]pyrrolo[1,2-*a*]quinoxaline (4j). A solution of **4a** (0.100 g, 0.30 mmol) in dry THF (0.6 mL) was added dropwise to a stirred solution of CDI (50.0 mg, 0.30 mmol) in dry THF (0.6 mL). The reaction mixture was stirred at room temperature for 30 min. Afterward it was heated under reflux for further 30 min and finally was allowed to cool to room temperature. Methanesulfonamide (29.0 mg, 0.30 mmol) was added in one portion to the reaction mixture which was stirred for 10 min before a solution of DBU (45.0 mg, 0.30 mmol) in dry THF (0.5 mL) was added dropwise. The mixture was stirred for a further 12 h and then concentrated to dryness. The residue was taken up with water (10 mL) and extracted with ethyl acetate (3 × 10 mL). The organic layer was washed with water, dried over sodium sulfate, and concentrated. Purification by flash chromatography (9:1 DCM/methanol) afforded, after recrystallization, compound **4j** (27.0 mg, 67%) as colorless prisms (mp 187−189 °C, *n*-hexane). ^{1}H NMR ($CDCl_3$) δ 2.83 (m, 4H), 3.11 (s, 3H), 3.27 (s, 2H), 3.98 (m, 4H), 6.82 (m, 2H), 7.03 (m, 1H), 7.46 (m, 1H), 7.71 (m, 1H), 7.82 (m, 1H); IR (KBr) 1631, 1083 cm^{-1}. Anal. ($C_{18}H_{20}N_5O_3SF$) C, H, N.

7-Fluoro-4-[4-(1*H*-tetrazol-5-yl)methylpiperazin-1-yl]pyrrolo[1,2-*a*]quinoxaline (4k). A mixture of **12** (0.100 g, 0.32 mmol), piperidine hydrochloride (97.0 mg, 0.80 mmol), and sodium azide (52.0 mg, 0.80 mmol) in anhydrous *N*,*N*-DMF (1 mL) was heated to 115 °C for 16 h. The reaction mixture was diluted with aqueous ammonium chloride (10 mL) and extracted with ethyl acetate (3 × 15 mL). The organic layers were washed with brine, dried over sodium sulfate, and concentrated. The residue was purified by flash chromatography (7:3 DCM/methanol) to give, after recrystallization, **4k** (28.0 mg, 69%) as pale-yellow prisms (mp 233−234 °C, *n*-hexane). ^{1}H NMR (DMSO-d_6) δ 2.70 (m, 4H), 3.74 (m, 4H), 3.88 (s, 2H), 6.81 (m, 1H), 6.96 (m, 1H), 7.19 (m, 2H), 8.17 (m, 2H), 8.32 (m, 1H); IR (Nujol) 3211−2405, 1628 cm^{-1}. Anal. ($C_{17}H_{17}N_8F$) C, H, N.

7-Fluoro-4-[4-(2,3-dihydro-4*H*-3-oxo-1,2,4-triazol-5-yl)methylpiperazin-1-yl]pyrrolo[1,2-*a*]quinoxaline (4l). A mixture of **10a** (0.500 g, 1.85 mmol), *N*-carbomethoxy-2-chloroacetamidrazone[16] (0.300 g, 1.850 mmol), and potassium carbonate (0.500 g, 3.700 mmol) in *N*,*N*-DMF (10 mL) was stirred at 70 °C for 18 h and at 140 °C for 1 h. After cooling to room temperature, the material was partitioned between ethyl acetate (15 mL) and water (5 mL). The organic layer was washed with water, dried over sodium sulfate, and concentrated. The residue was purified by flash chromatography (95:5 ethyl acetate/methanol) and recrystallized from ethyl acetate

to give **4l** (0.137 g, 75%) as colorless prisms (mp 169−171 °C, *n*-hexane). ^{1}H NMR (DMSO-d_6) δ 2.59 (m, 4H), 3.31 (s, 2H), 3.85 (m, 4H), 6.78 (m, 1H), 6.97 (m, 1H), 7.15 (m, 1H), 7.29 (m, 1H), 8.16 (m, 1H), 8.32 (m, 1H), 10.15 (br, 1H), 11.32 (br, 1H); IR (Nujol) 1698 cm^{-1}. Anal. ($C_{18}H_{18}N_7OF$) C, H, N.

5-[4-(7-Fluoropyrrolo[1,2-*a*]quinoxalin-4-yl)-piperazin-1-ylmethyl]-3*H*-[1,3,4]oxadiazol-2-one (4m). Compound **11a** (0.100 g, 0.28 mmol) was dissolved in hydrazine hydrate (8.4 mL) and heated to 120 °C for 2 h. After cooling to room temperature, the mixture was evaporated under reduced pressure. The residue was treated with water (10 mL) and extracted with ethyl acetate (3 × 15 mL). The crude product was purified by flash chromatography (9:1 DCM/methanol) to give, after recrystallization, [4-(7-fluoropyrrolo[1,2-*a*]quinoxalin-4-yl)piperazin-1-yl]acetic acid hydrazide (84.0 mg, 88%) as colorless prisms (mp 165−167 °C, *n*-hexane). ^{1}H NMR (DMSO-d_6) δ 2.62 (m, 4H), 3.02 (s, 2H), 3.78 (m, 4H), 4.26 (br, 2H), 6.80−6.98 (m, 2H), 7.12−7.28 (m, 2H), 8.15 (m, 1H), 8.31 (m, 1H), 9.01 (br, 1H); IR (Nujol) 1695, 1598 cm^{-1}. CDI (0.144 g, 0.87 mmol) was added to a solution of the above compound (0.200 g, 0.58 mmol) and triethylamine (160 μL, 1.15 mmol) in THF (6 mL), cooled to 0 °C. The reaction mixture was stirred at room temperature for 12 h. The volatiles were removed in vacuo, and the residue was dissolved in diethyl ether. The organic phase was washed with a saturated solution of sodium bicarbonate and with brine. The organic layer was dried over sodium sulfate and concentrated in vacuo. The resulting white solid was purified by flash chromatography (2:1 *n*-hexane/ethyl acetate) to afford, after recrystallization, **4m** (0.102 g, 48%) as colorless prisms (mp 151−153 °C, *n*-hexane). ^{1}H NMR (acetone-d_6) δ 2.75 (m, 4H), 3.59 (s, 2H), 3.84 (m, 4H), 6.77 (m, 1H), 6.95 (m, 1H), 7.05 (m, 1H), 7.25 (m, 1H), 8.01 (m, 1H), 8.12 (m, 1H), 11.33 (br, 1H); IR (Nujol) 1785 cm^{-1}. Anal. ($C_{18}H_{17}N_6O_2F$) C, H, N.

(*S*)-{2-[4-(7-Fluoropyrrolo[1,2-*a*]quinoxalin-4-yl)piperazin-1-yl]-1-hydroxymethyl-2-oxoethyl}carbamic Acid *tert*-Butyl Ester ((*S*)-(13)). *N*-(*tert*-Butoxycarbonyl)-L-serine (0.231 g, 1.13 mmol), 1-hydroxybenzotriazole (0.152 g, 1.13 mmol), and *N*-methylmorpholine (60 μL, 0.54 mmol) were added to a stirred solution of **10a** (0.200 g, 0.75 mmol) in *N*,*N*-DMF (6 mL). The resulting mixture was cooled to 0 °C and treated with 1-ethyl-3-[3-(dimethylamino)propyl]carbodiimide hydrochloride (0.115 g, 0.59 mmol). After being stirred at room temperature for 18 h, the mixture was poured into a saturated solution of sodium bicarbonate and the aqueous layer was extracted with ethyl acetate (3 × 20 mL). The organic phase was washed with water and brine, dried over sodium sulfate, and evaporated. The residue was purified by flash chromatography (ethyl acetate) to afford, after recrystallization, compound (*S*)-**13** (0.220 g, 63%) as colorless prisms (mp 182−183 °C, *n*-hexane). ^{1}H NMR ($CDCl_3$) δ 1.45 (s, 9H), 3.78 (m, 5H), 3.87 (m, 6H), 4.68 (m, 1H), 5.76 (br, 1H), 6.77 (m, 2H), 7.02 (m, 1H), 7.39 (m, 1H), 7.66 (m, 1H), 7.77 (m, 1H); IR (chloroform) 1695, 1093 cm^{-1}.

(*S*)-2-Amino-3-[4-(7-fluoropyrrolo[1,2-*a*]quinoxalin-4-yl)piperazin-1-yl]propionic Acid ((*S*)-4n). *N*-(*tert*-Butyloxycarbonyl)-L-serine β-lactone[17] (50.0 mg, 0.27 mmol) was added to a vigorously stirred solution of **10a** (0.200 g, 0.82 mmol) in dry *N*,*N*-DMF (8 mL). The resulting mixture was stirred at room temperature for 12 h, then was evaporated under reduced pressure, and trifluoracetic acid (0.68 mL) was added to the residue with ice-cooling. The resulting mixture was stirred at room temperature for 12 h. Excess trifluoracetic acid was removed under reduced pressure, and the residue was applied to a column of Dowex 50WX8400 resin. The column was washed with 50% aqueous ethanol and eluted with 1 M aqueous pyridine. The ninhydrin-positive fractions of the 1 M aqueous pyridine eluate were combined and evaporated to dryness. Treatment of the residue with 1 N hydrochloric acid afforded the hydrochloride salt of (*S*)-**4n** as an off-white solid in 83% yield (mp 278−279 °C, *n*-hexane). ^{1}H NMR (D_2O) δ 3.65 (m, 6H), 4.38 (m, 5H), 7.09 (m, 1H), 7.28 (m, 1H), 7.46 (m, 1H), 7.62 (m, 1H), 7.93 (m, 1H), 8.31 (m, 1H); IR (Nujol) 1486, 1628 cm^{-1}. $[\alpha]_D^{24}$ +9.7 (*c* 0.6, H_2O). Anal. ($C_{18}H_{20}N_5O_2F$) C, H, N.

(*R*)-2-Amino-3-[4-(7-fluoropyrrolo[1,2-*a*]quinoxalin-4-yl)piperazin-1-yl]propionic Acid ((*R*)-4n). From **10a** and *N*-(*tert*-butyloxycarbonyl)-D-serine β-lactone[17] the title compound was prepared following the procedure described for (*S*)-**4n** and was obtained, after recrystallization, as colorless prisms. Spectroscopic and physical data were identical to those of the (*S*)-enantiomer; $[\alpha]_D^{24}$ −10.5 (*c* 0.5, H_2O). Anal. ($C_{18}H_{20}N_5O_2F$) C, H, N.

(*S*)-2-Amino-1-[4-(7-fluoropyrrolo[1,2-*a*]quinoxalin-4-yl)piperazin-1-yl]-3-hydroxypropan-1-one ((*S*)-4o). The Boc-protected product (*S*)-**13** (0.120 g, 0.34 mmol) was treated with an excess of trifluoracetic acid (3 mL), and the resulting solution was stirred at room temperature for 30 min. Excess of trifluoroacetic acid was removed under vacuum. The hydrochloride salt was generated by stirring an aqueous solution of the trifluoroacetate salt with IRA400 Amberlyte resin in its Cl^- form during 24 h at room temperature. The resin was removed by filtration, and the aqueous solution was washed twice with ethyl acetate. Lyophilization afforded the pure hydrochloride salt in 86% yield (mp 176−177 °C, *n*-hexane). ^{1}H NMR (D_2O) δ 4.05 (m, 6H), 4.29 (m, 4H), 4.71 (m, 1H), 7.02 (m, 1H), 7.19 (m, 1H), 7.43 (m, 1H), 7.57 (m, 1H), 7.83 (m, 1H), 8.18 (m, 1H); IR (Nujol) 1698, 1598, 1088 cm^{-1}; $[\alpha]_D^{24}$ −14.3 (*c* 0.6, H_2O). Anal. ($C_{18}H_{20}N_5O_2F$) C, H, N.

(4-Quinolin-2-yl-piperazin-1-yl)acetic Acid Ethyl Ester (14). DIPEA (0.180 g, 1.400 mmol) and ethyl bromoacetate (0.260 g, 1.50 mmol) were added to a solution of **1** (0.200 g, 0.94 mmol) in acetonitrile (15 mL). The mixture was stirred at room temperature for 12 h. The solvent was evaporated, and the residue was dissolved in DCM and washed with water. The organic phase was dried over sodium sulfate and evaporated. The residue was purified by flash chromatography (1:1 *n*-hexane/ethyl acetate) to give, after recrystallization, compound **14** (0.260 g, 93%) as colorless prisms (mp 205−207 °C, *n*-hexane). ^{1}H NMR ($CDCl_3$) δ 1.26 (t, 3H, J = 7.1 Hz), 2.81 (m, 4H), 3.41 (s, 2H), 3.98 (m, 4H), 4.24 (q, 2H, J = 7.1 Hz), 6.92 (m, 1H), 7.23 (m, 1H), 7.59 (m, 2H), 7.75 (m, 1H), 7.91 (m, 1H); IR (Nujol) 1728 cm^{-1}.

(4-Quinolin-2-ylpiperazin-1-yl)acetic Acid (15). A solution of lithium hydroxide (20.0 mg, 0.60 mmol) in water (3 mL) was added dropwise to a solution of **14** (0.150 g, 0.50 mmol) in THF (3 mL). The mixture was stirred at room temperature for 1 h. Then the mixture was concentrated to dryness and the residue was dissolved in water (1 mL). The aqueous phase was acidified to pH 5 with 1 N hydrochloric acid and extracted with ethyl acetate (3 × 10 mL). The organic layer was washed with water, dried over sodium sulfate, and evaporated. The residue was purified by flash chromatography (ethyl acetate) to give, after recrystallization, **15** (88.0 mg, 65%) as colorless prisms (mp 230 °C dec, *n*-hexane). ^{1}H NMR (DMSO-d_6) δ 2.75 (m, 4H), 3.35 (s, 2H), 3.76 (m, 4H), 7.21 (m, 2H), 7.51 (m, 2H), 7.65 (m, 1H), 7.98 (m, 1H), 9.81 (br, 1H); IR (Nujol) 1702 cm^{-1}. Anal. ($C_{15}H_{17}N_3O_2$) C, H, N.

Binding Assays. 5-HT Receptor Subtypes. Binding assays were performed according to previously reported experimental procedures.[12,13,41]

Dopamine, Adrenergic, and Muscarinic Receptors. Binding assays were performed according to previously reported experimental procedures.[42−44]

Molecular Modeling. All molecular modeling studies were performed on SGI Octane2 2XR14000 workstation. The log *D* values together with single and apparent pK_a of all possible tautomers of compounds **1**, **4a**−**o**, **5a**,**b**, **6a**,**b**, and **15** were calculated by using the pK_a DB program in the LogD Sol suite, v10.0 (Advanced Chemistry Development Inc., Toronto, Canada). The percentage of neutral/ionized forms at physiological pH (7.2) was computed with the Solubility DB program within the same software suite according to calculated apparent pK_a.

All possible tautomers of compounds **4a**−**o** and **15** were built in the calculated most abundant ionic form at pH 7.2 by using the Insight2005 Builder module (Accelrys, San Diego, CA). Compounds **4a** and **4k** were also modeled in the neutral and zwitterionic form, respectively. On the bases of R′ single pK_a values, compounds **4a**−**o** and **15** were clustered in two groups: group A (pK_a < 7) and group B (pK_a > 7). Conformational space was sampled through

200 cycles of simulated annealing (CVFF force field[45]) by following our standard protocol. An initial temperature of 1000 K was applied to the system for 1000 fs with the aim of surmounting torsional barriers; successively temperature was linearly reduced to 300 K with a decrement of 0.5 K/fs. Resulting structures were subjected to energy minimization within the Insight2005 Discover module (CVFF force field, conjugate gradient algorithm;[46] $\varepsilon = 80r$) until the maximum rms derivative was less than 0.001 kcal/Å. The structures were subsequently ranked by their conformational energy values. Resulting conformers were then subjected to an in depth structural analysis and accordingly grouped into families. The following structural parameters were measured: (i) distance between the protonatable nitrogen (N-4) and the H-bond acceptor group (N-1); (ii) distance between the center of the aromatic ring (X1) and N-4; (iii) distance between X1 and N-1; (iv) distance between N-4 and the plane of the aromatic ring; (v) distance between the proton on N-4 and the closest negatively charged atom on R′ for cluster A or (vi) distance between the exchangeable hydrogen on R′ and N-4 for cluster B; (vii) distance between the proton on N-4 and N-1 for cluster A or (viii) distance between N-1 and the exchangeable hydrogen on R′ for cluster B; (ix) distance between the proton on N-4 and X1 for cluster A or (x) distance between X1 and the exchangeable hydrogen on R′ for cluster B. In particular, parameters iv−x were used for structural classification into families.

All MM conformers were successively submitted to 1SCF, AM1 energy calculation in the Mopac 6.0[47a] package in Ampac/Mopac module of Insight2000.1 and ranked by resulting conformational energies.

MM global minima together with the lowest AM1 energy conformer of each family were selected to be successively subjected to a full geometry optimization by semiempirical calculations, using the quantum mechanical method AM1 implemented in the Mopac 2007.[47b] The EF optimization method (DDMAX = 0.05) and the Pulay convergence method (GNORM = 0.01) have been used. To reach a full geometry optimization, the criterion for terminating all optimizations was increased by a factor of 100, using the keyword PRECISE. ESP charges were computed in addition to default Coulson atomic charges, by adding the keywords ESP and STO3G.

The electrostatic potentials of AM1 conformers, including ESP charges, were also calculated by the MNDO semiempirical method (1 SCF).

Resulting structures were tabulated, analyzed, and grouped into families following the same geometric criteria described above.

Functional in Vitro Studies. Compounds were checked at increasing doses for evaluating the percent decrease of developed tension on isolated left atrium driven at 1 Hz (positive inotropic activity), the percent increase in atrial rate on spontaneously beating right atrium (positive chronotropic activity). Increase in vascular contraction was evaluated on guinea pig aortic strips. Data were analyzed by Student's *t*-test. The agonistic potency of compounds was defined as EC_{50}, and IC_{50} was evaluated from log concentration−response curves (Probit analysis by Litchfield and Wilcoxon[48] or GraphPad Prism software[49,50]) in the appropriate pharmacological preparations. The biological results are expressed as pD_2. All data are presented as mean ± SEM.[50]

5-HT subtypes blocking activity was assessed by antagonism of 5-HT-induced positive heart rate in guinea pig spontaneously beating right. Data were analyzed by Student's *t*-test. The criterion for significance was a $P < 0.05$. IC_{50} values for noncompetitive antagonism were calculated from log concentration−response curves by Probit analysis.[48] The biological results are expressed as pIC_{50}. The competitive antagonist activity of tropisetron was expressed as pA_2. All data are presented as mean values ± SEM.

Guinea Pig Atrial Preparations. Female guinea pigs (300−400 g) were sacrificed by cervical dislocation. After thoracotomy the heart was immediately removed and washed by perfusion through the aorta with oxygenated Tyrode solution of the following composition (mM): 136.9 NaCl, 5.4 KCl, 2.5 $CaCl_2$, 1.0 $MgCl_2$, 0.4 $NaH_2PO_4 \cdot H_2O$, 11.9 $NaHCO_3$, and 5.5 glucose. Ketanserin (1 μM) was also added to Tyrode solution to exclude any action at 5-HT_2R. The physiological salt solution (PSS) was buffered at pH 7.4 by saturation with 95% O_2−5% CO_2 gas, and the temperature was maintained at 35 °C. Isolated guinea pig heart preparations were used, spontaneously beating right and left atria driven at 1 Hz. For each preparation, the entire left and right atria were dissected from the ventricles, cleaned of excess tissue, and hung vertically in a 15 mL organ bath containing the PSS continuously bubbled with 95% O_2−5% CO_2 gas at 35 °C, pH 7.4. The contractile activity was recorded isometrically by means of a force transducer (FT 0.3, Grass Instruments Corporation, Quincy, MA) using Power Lab software (AD-Instruments Pty Ltd., Castle Hill, Australia). The left atrium was stimulated by rectangular pulses of 0.6−0.8 ms duration and about 50% threshold voltage through two platinum contact electrodes in the lower holding clamp (Grass S88 stimulator). The right atrium was in spontaneous activity. After the tissue was beating for several minutes, a length−tension curve was determined, and the muscle length was maintained at the length that elicited 90% of maximum contractile force observed at the optimal length. A stabilization period of 45−60 min was allowed before the atria were used to test compounds. During the equilibration period, the bathing solution was changed every 15 min and the threshold voltage was ascertained for the left atrium. Atrial muscle preparations were used to examine the inotropic and chronotropic activity of the compounds (0.1, 0.5, 1, 5, 10, 50, and 100 μM), first dissolved in dimethyl sufoxide (DMSO) and then diluted with PSS. According to this procedure, the concentration of DMSO in the bath solution never exceeded 0.3%, a concentration that did not produce appreciable inotropic and chronotropic effects. During the construction of cumulative dose−response curves, the next higher concentration of the compounds was added only after the preparation reached a steady state.

Guinea Pig Aortic Strips. The thoracic aorta was removed and placed in Tyrode solution of the following composition (mM): 118 NaCl, 4.75 KCl, 2.54 $CaCl_2$, 1.20 $MgSO_4$, 1.19 KH_2PO_4, 25 $NaHCO_3$, and 11 glucose equilibrated with 95% O_2−5% CO_2 gas at pH 7.4. The vessel was cleaned of extraneous connective tissue. Two helicoidal strips (10 mm × 1 mm) were cut from each aorta beginning from the end most proximal to the heart. Vascular strips were then tied with surgical thread (6−0) and suspended in a jacketed tissue bath (15 mL) containing aerated PSS at 35 °C. Strips were secured at one end to a force displacement transducer (FT 0.3, Grass Instruments Corporation) for monitoring changes in isometric contraction. Aortic strips were subjected to a resting force of 1 g and washed every 20 min with fresh PSS for 1 h. After the equilibration period the compounds (0.1, 0.5, 1, 5, 10, 50, and 100 μM) were added cumulatively to the bath allowing for any contraction for obtaining an equilibrated level of force. Addition of the drug vehicle had no appreciable effect on induced contraction (DMSO for all compounds).

Functional Antagonism. The right atrium from guinea pig, removed and prepared as described above, was equilibrated for 1 h, and cumulative concentration−response curves to 5-HT (0.001−1.0 μM) were constructed. The concentration of agonist in the organ bath was increased approximately 5-fold at each step, with each addition being made only after the response to the previous addition had attained a maximal level and remained steady. During the equilibration period the bathing solution was changed every 15 min. Following incubation with the antagonist for 30 min, a new concentration−response curve to 5-HT was obtained. Parallel experiments in which tissues did not receive any antagonist were run in order to check any variation in sensitivity.

Functional in Vivo Studies. von Bezold−Jarisch Reflex. Adult male Sprague−Dawley rats (250−300 g body weight, Centre d'Elevage R. Janvier, Le Genest, France) were anesthetized with urethane (1.6 g/kg ip), and a tracheotomy was performed to insert an endotracheal tube. A catheter (0.3 mm internal diameter) was inserted into the abdominal aorta via the femoral artery in order to record the arterial pressure and heart rate. A femoral vein was exposed and cannulated for iv injection of drugs. The von B-J reflex (which consists of a 64% drop in heart rate within 30 s following the injection of 40 μg/kg (iv) of PBG) was measured 5, 15, and 30

min after the iv administration of various doses of each tested compound administered alone (agonist effect) or 5 min before PBG (antagonist effect). Under these conditions, 1 μg/kg (iv) of zacopride injected 5 min before PBG completely prevented PBG-evoked bradycardia.[38]

Brain-to-Plasma Distribution Studies. Animals and Treatment. Male CD1 albino mice, 25−30 g (Charles River, Italy), were used. Procedures involving animals and their care were conducted in conformity with the institutional guidelines that are in compliance with national (D.L., No. 116, G.U., Suppl. 40, 18 Febbraio 1992, Circolare No. 8, G.U., 14 Luglio 1994) and international laws and policies (EEC Council Directive 86/609, 0J L358, 1, Dec 12, 1987; Guide for the Care and Use of Laboratory Animals).

Animals were injected with 5 and 20 mg/kg (*S*)-**4n** (as hydrochloride salt) and sacrificed by decapitation at various times thereafter for parallel determination of the compound in plasma and whole brain. Mixed arteriovenous trunk blood was collected in heparinized tubes and centrifuged at 3000*g* for 10 min, and the plasma was stored at −20 °C. Brain was immediately removed, blotted with paper for removing excess surface blood, and quickly frozen in dry ice.

Compound (*S*)-**4n** was extracted from plasma and brain homogenate by a solid−liquid extraction procedure and quantified by HPLC with UV detection (240 nm). Briefly, 0.8 mL of 0.01 M phosphate buffer, pH 7.4, and 50 μL of a solution of **7b** (IS)[13] in methanol (5 μg/mL) were added to 0.2 mL of plasma and the samples were added to Sep-Pac Vac C18 cartridges (contains 100 mg of sorbent), prewetted with 1 mL of methanol and 1 mL of water. Cartridges were washed with 1 mL of water and 0.2 mL of methanol. The compound was removed by eluting the cartridges with 1 mL of methanol, which was evaporated to dryness. The residue was dissolved in the mobile phase (methanol/0.01 M KH_2PO_4 (50:50, v/v) buffered to pH 4.6 with 0.175 M phosphoric acid) and injected into the HPLC column (μBondpack C18, 30 cm × 4.6 mm i.d., 10 μm). The retention times were 14 min for compound (*S*)-**4n** and 23 min for the IS.

Brain tissue was homogenized (10 mL/g) in 0.01 M phosphate buffer, pH 7.4, and methanol (60:40 v/v) and centrifuged at 9000*g* for 15 min (at 4 °C). The residue was reconstituted in 1 mL of the same solution and recentrifuged. The combined supernatants were processed as described for plasma. The lower limits for quantification of (*S*)-**4n** in plasma were about 0.25 nmol/mL using 0.2 mL; in brain the limit was about 0.5 nmol/g, using 1 mL of brain homogenate or approximately 100 mg of tissue. At these concentrations the coefficients of variation (CV) for the precision and reproducibility of the assay were between 15% and 20%. Higher concentrations gave CV between 5% and 9%.

Acknowledgment. The authors thank MIUR (Roma) for financial support (PRIN).

Supporting Information Available: Tables of pharmacophoric distances, features, partial charges, structural comparison, calculated log *D* values, and elemental analysis results; figures showing agonists and antagonists and superimpositions. This material is available free of charge via the Internet at http://pubs.acs.org.

References

(1) Dukat, M.; Choi, Y. N.; Teitler, M.; Du Pre, A.; Herrick-Davis, K.; Smith, C.; Glennon, R. A. The binding of arylguanidines at 5-HT$_3$ serotonin receptors: a structure−affinity investigation. *Bioorg. Med. Chem. Lett.* **2001**, *11*, 1599–1603.

(2) Thompson, A. J.; Lummis, S. C. R. The 5-HT$_3$ receptors as therapeutic target. *Expert Opin. Ther. Targets* **2007**, *11*, 527–540.

(3) Collingridge, G. L.; Olsen, R. W.; Peters, J.; Spedding, M. A nomenclature for ligand-gated ion channels. *Neuropharmacology* **2009**, *56*, 2–5.

(4) Niesler, B.; Walstab, J.; Combrink, S.; Moeller, D.; Kapeller, J.; Rietdorf, J.; Boenisch, H.; Gothert, M.; Rappold, G.; Bruess, M. Characterization of the novel human serotonin receptor subunits 5-HT$_3$C, 5-HT$_3$D and 5-HT$_3$E. *Mol. Pharmacol.* **2007**, *72*, 8–16.

(5) Barnes, N. M.; Hales, T. G.; Lummis, S. C. R.; Peters, J. A. The 5-HT$_3$ receptor, the relationship between structure and function. *Neuropharmacology* **2009**, *56*, 273–284.

(6) Faerber, L.; Drechsler, S.; Ladenburge, S.; Gschaidmeier, H.; Fischer, W. The neuronal 5-HT$_3$ receptor network after 20 years of research. Evolving concepts in management of pain and inflammation. *Eur. J. Pharmacol.* **2007**, *560*, 1–8.

(7) Stevens, R.; Rusch, D.; Solt, K.; Raines, D. E.; Davies, P. A. Modulation of human 5-hydroxytriptamine type 3AB receptors by volatile anesthetics and alcohols. *J. Pharmacol. Exp. Ther.* **2005**, *314*, 338–345.

(8) Krzywkowski, K.; Davies, P. A.; Irving, A. J.; Bräuner-Osborne, H.; Jensen, A. A. Characterization of the effects of four HTR3B polymorphisms on human 5-HT3AB receptor expression and signalling. *Pharmacogenet. Genomics* **2008**, *18*, 1027–1040, and references cited therein.

(9) Ramage, A. G.; Villalón, C. M. 5-Hydroxytryptamine and cardiovascular regulation. *Trends Pharmacol. Sci.* **2008**, *29*, 472–481.

(10) Nishio, H.; Fujii, A.; Nakata, Y. Re-examination for pharmacological properties of serotonin-induced tachycardia in isolated guinea-pig atrium. *Behav. Brain Res.* **1996**, *73*, 301–304.

(11) Ito, H.; Kiso, T.; Kamato, T.; Yuki, H.; Akuzawa, S.; Nagakura, Y.; Yamano, M.; Suzuki, M.; Naitoh, Y.; Sakai, H.; Iwaoka, K.; Yamaguchi, T. Pharmacological profile of YM-31636, a novel 5-HT$_3$ receptor agonist, in vitro. *Eur. J. Pharmacol.* **2000**, *409*, 195–201.

(12) Campiani, G.; Cappelli, A.; Nacci, V.; Anzini, M.; Vomero, S.; Hamon, M.; Cagnotto, A.; Fracasso, C.; Uboldi, C.; Caccia, S.; Consolo, S.; Mennini, T. Novel and highly potent 5-HT$_3$ receptor agonists based on a pyrroloquinoxaline structure. *J. Med. Chem.* **1997**, *40*, 3670–3678.

(13) Campiani, G.; Morelli, E.; Gemma, S.; Nacci, V.; Butini, S.; Hamon, M.; Novellino, E.; Greco, G.; Cagnotto, A.; Goegan, M.; Cervo, L.; Dalla Valle, F.; Fracasso, C.; Caccia, S.; Mennini, T. Pyrroloquinoxaline derivatives as high-affinity and selective 5-HT$_3$ receptor agonists: synthesis, further structure−activity relationships, and biological studies. *J. Med. Chem.* **1999**, *42*, 4362–4379.

(14) Castan, F.; Schambel, P.; Enrici, A.; Rolland, F.; Bigg, D. C. H. New arylpiperazine derivatives with high affinity for 5-HT$_3$ receptor sites. *Med. Chem. Res.* **1996**, *6*, 81–101.

(15) Cappelli, A.; Gallelli, A.; Manini, M.; Anzini, M.; Mennuni, L.; Makovec, F.; Menziani, M. C.; Alcaro, S.; Ortuso, F.; Vomero, S. Further studies on the interaction of the 5-hydroxytryptamine$_3$ (5-HT$_3$) receptor with arylpiperazine ligands. Development of a new 5-HT$_3$ receptor ligand showing potent acetylcholinesterase inhibitory properties. *J. Med. Chem.* **2005**, *48*, 3564–3575.

(16) Yanagisava, I.; Hirata, Y.; Ishii, Y. Histamine H$_2$ receptor antagonists. Synthesis of *N*-cyano and carbamoyl amidine derivatives and their biological activities. *J. Med. Chem.* **1984**, *27*, 849–857.

(17) Arnold, L. D.; Kalantar, T. H.; Vederas, J. C. Conversion of serine to stereochemically pure β-substituted α-amino acids via β-lactones. *J. Am. Chem. Soc.* **1985**, *107*, 7105–7109.

(18) (a) Gaster, L. M.; King, F. D. Serotonin 5-HT$_3$ and 5-HT$_4$ receptor antagonists. *Med. Res. Rev.* **1997**, *17*, 163–214, and references therein. (b) Hibert, M. F.; Hoffman, R.; Miller, R. C.; Carr, A. C. Conformation−activity relationship study of 5-HT$_3$ receptor antagonists and a definition of a model for this receptor site. *J. Med. Chem.* **1990**, *33*, 1594–1600. (c) Evans, S. M.; Galdes, A.; Gall, M. Molecular modeling of 5-HT$_3$ receptor ligands. *Pharmacol., Biochem. Behav.* **1991**, *40*, 1033–1040. (d) Swain, C. J.; Baker, R.; Kneen, C.; Moseley, J.; Saunders, J.; Seward, E. M.; Stevenson, G. I.; Staunton, J.; Watling, K. Novel 5-HT$_3$ antagonists. Indole oxadiazoles. *J. Med. Chem.* **1991**, *34*, 140–151. (e) Turconi, M.; Nicola, M.; Quintero, M. G.; Maiocchi, L.; Micheletti, R.; Giraldo, E.; Donetti, A. Synthesis of a new class of 2,3-dihydro-2-oxo-1*H*-benzimidazole-1-carboxylic acid derivatives as highly potent 5-HT$_3$ receptor antagonists. *J. Med. Chem.* **1990**, *33*, 2101–2108. (f) Clark, R. D.; Miller, A. B.; Berger, J.; Repke, D. B.; Weinhardt, K. K.; Kowalczyk, B. A.; Eglen, R. M.; Bonhaus, D. W.; Lee, C. H.; Michel, A. D.; Smith, W. L.; Wong, E. H. F. 2-(Quinuclidin-3-yl)pyrido[4,3-*b*]indol-1-ones and isoquinolin-1-ones. Potent conformationally restricted 5-HT$_3$ receptor antagonists. *J. Med. Chem.* **1993**, *36*, 2645–2657. (g) Whelan, B. A.; Iriepa, I.; Galvez, E.; Orjales, A.; Berisa, A.; Labeaga, L.; Garcia, A. G.; Uceda, G.; Sanz-Aparicio, J.; Fonseca, I. Synthesis and structural, conformational, biochemical, and pharmacological study of new compounds derived from tropane-3-spiro-4′(5′)-imidazoline as potential 5-HT$_3$ receptor antagonists. *J. Pharm. Sci.* **1995**, *84*, 101–106. (h) Gouldson, P. R.; Winn, P. J.; Reynolds, C. A. A molecular dynamics approach to receptor mapping: application to the 5HT$_3$ and β2-adrenergic receptors. *J. Med. Chem.* **1995**, *38*, 4080–4086. (i) Glennon, R. A.; Westkaemper, R. B.; Bartyzel, P. Medicinal Chemistry of Serotonergic Agents. In *Serotonin Receptor Subtypes: Basic & Clinical Aspects*; Peroutka, S. J., Ed.; Wiley-Liss: New York, 1990; *Recept.*

Biochem. Method. Ser. **1990**, *15*; 19−64. (j) Yamada, M.; Sato, Y.; Kobayahi, K.; Konno, F.; Soneda, T.; Watanabe, T. A new 5-HT_3 receptor ligand. II. Structure−activity analysis of 5-HT_3 receptor agonist activity in the gut. *Chem. Pharm. Bull.* **1998**, *46*, 445–451.

(19) Steward, L. J.; Boess, F. G.; Steele, J. A.; Liu, D.; Wong, N.; Martin, I. L. Importance of phenylalanine 107 in agonist recognition by the 5-hydroxytryptamine(3A) receptor. *Mol. Pharmacol.* **2000**, *57*, 1249–1255.

(20) Sullivan, N. L.; Thompson, A. J.; Price, K. L.; Lummis, S. C. Defining the roles of Asn-128, Glu-129 and Phe-130 in loop A of the 5-HT_3 receptor. *Mol. Membr. Biol.* **2006**, *23*, 442–451.

(21) Venkataraman, P.; Venkatachalan, S. P.; Joshi, P. R.; Muthalagi, M.; Schulte, M. K. Identification of critical residues in loop E in the 5-HT_{3AS}R binding site. *BMC Biochem.* **2002**, *3*, 15.

(22) Price, K. L.; Lummis, S. C. The role of tyrosine residues in the extracellular domain of the 5-hydroxytryptamine3 receptor. *J. Biol. Chem.* **2004**, *279*, 23294–23301.

(23) Joshi, P. R.; Suryanarayanan, A.; Hazai, E.; Sculte, M. K.; Maksay, G.; Bikadi, Z. Interactions of granisetron with an agonist-free 5-HT_{3A} receptor model. *Biochemistry* **2006**, *45*, 1099–1105.

(24) Venkataraman, P.; Joshi, P. R.; Venkatachalan, S. P.; Muthalagi, M.; Parihar, H. S.; Kirschbaum, K. S.; Schulte, M. K. Functional group interactions of a 5-HT_3R antagonist. *BMC Biochem.* **2002**, *3*, 16.

(25) Cappelli, A.; Anzini, M.; Vomero, S.; Mennuni, L.; Makovec, F.; Hamon, M.; De Benedetti, P. G.; Menziani, M. C. The interactions of the 5-HT(3) receptor with arylpiperazine, tropane, and quinuclidine ligands. *Curr. Top. Med. Chem.* **2002**, *2*, 599–624.

(26) Menziani, M. C.; De Rienzo, F.; Cappelli, A.; Anzini, M.; De Benedetti, P. G. A computational model of the 5-HT_3 receptor extracellular domain: a search for ligand binding sites. *Theor. Chem. Acc.* **2001**, *106*, 98–104.

(27) Maksay, G.; Simonyi, M.; Bikadi, Z. Subunit rotation models activation of serotonin 5-HT_{3AB} receptors by agonists. *J. Comput.-Aided Mol. Des.* **2004**, *18*, 651–664.

(28) Reeves, D. C.; Sayed, M. F.; Chau, P. L.; Price, K. L.; Lummis, S. C. Prediction of 5-HT_3 receptor agonist-binding residues using homology modelling. *Biophys. J.* **2003**, *84*, 2338–2344.

(29) Boess, F. G.; Steward, L. J.; Steele, J. A.; Liu, D.; Reid, J.; Glencorse, T. A.; Martin, I. L. Analysis of the ligand binding site of the 5-HT_3 receptor using site directed mutagenesis: importance of glutamate 106. *Neuropharmacology* **1997**, *36*, 637–647.

(30) Beene, D. L.; Brandt, G. S.; Zhong, W.; Zacharias, N. M.; Lester, H. A.; Dougherty, D. A. Cation-interactions in ligand recognition by serotonergic (5-HT_{3A}) and nicotinic acetylcholine receptors: the anomalous binding properties of nicotine. *Biochemistry* **2002**, *41*, 10262–10269.

(31) Maksay, G.; Bikadi, Z.; Simonyi, M. Binding interactions of antagonists with 5-hydroxytryptamine3A receptor models. *J. Recept. Signal Transduction Res.* **2003**, *23*, 255–270.

(32) Yan, D.; White, M. M. Spatial orientation of the antagonist granisetron in the ligand-binding site of the 5-HT_3 receptor. *Mol. Pharmacol.* **2005**, *68*, 365–371.

(33) Zhu, L. P.; Ye, D. Y.; Tang, Y. Structure-based 3D-QSAR studies on thiazoles as 5-HT_3 receptor antagonists. *J. Mol. Model.* **2007**, *13*, 121–131.

(34) Yan, D.; Schulte, M. K.; Bloom, K. E.; White, M. M. Structural features of the ligand-binding domain of the serotonin 5HT_3 receptor. *J. Biol. Chem.* **1999**, *274*, 5537–5541.

(35) Thompson, A. J.; Price, K. L.; Reeves, D. C.; Chan, S. L.; Chau, P. L.; Lummis, S. C. Locating an antagonist in the 5-HT_3 receptor binding site using modelling and radioligand binding. *J. Biol. Chem.* **2005**, *280*, 20476–20482.

(36) Spier, A. D.; Lummis, S. C. The role of tryptophan residues in the 5-HT_3 receptor ligand binding domain. *J. Biol. Chem.* **2000**, *275*, 5620–5625.

(37) Suryanarayanan, A.; Joshi, P. R.; Bikádi, Z.; Mani, M.; Kulkarni, T. R.; Gaines, C.; Schulte, M. K. The loop C region of the murine 5-HT_{3A} receptor contributes to the differential actions of 5-hydroxytryptamine and *m*-chlorophenylbiguanide. *Biochemistry* **2005**, *44*, 9140–9149.

(38) Cohen, M. L.; Bloomquist, W.; Gidda, J. S.; Lacefield, W. Comparison of the 5-HT_3 receptor antagonist properties of ICS 205-930, GR38032F and Zacopride. *J. Pharmacol. Exp. Ther.* **1989**, *248*, 197–201.

(39) Caccia, S.; Garattini, S. Formation of active metabolites of psychotropic drugs. An updated review of their significance. *Clin. Pharmacokinet.* **1990**, *18*, 434–459.

(40) Caccia, S. N-Dealkylation of 1-arylpiperazine derivatives: disposition and metabolism of the 1-arylpiperazines formed. *Curr. Drug Metab.* **2007**, *8*, 612–622.

(41) Anzini, M.; Cappelli, A.; Vomero, S.; Giorgi, G.; Langer, T.; Hamon, H.; Merahi, N.; Emerit, B. M.; Cagnotto, A.; Skorupska, M.; Mennini, T.; Pinto, J. C. Novel, potent, and selective 5-HT_3 receptor antagonists based on the arylpiperazine skeleton: synthesis, structure, biological activity, and comparative molecular field analysis studies. *J. Med. Chem.* **1995**, *38*, 2692–2704.

(42) Campiani, G.; Butini, S.; Gemma, S.; Nacci, V.; Fattorusso, C.; Catalanotti, B.; Giorgi, G.; Cagnotto, A.; Goegan, M.; Mennini, T.; Minetti, P.; Di Cesare, M. A.; Mastroianni, D.; Scafetta, N.; Galletti, B.; Stasi, M. A.; Castorina, M.; Pacifici, L.; Ghirardi, O.; Tinti, O.; Carminati, P. Pyrrolo[1,3]benzothiazepine-based atypical antipsychotic agents. Synthesis, structure−activity relationship, molecular modeling, and biological studies. *J. Med. Chem.* **2002**, *45*, 344–359.

(43) Campiani, G.; Butini, S.; Trotta, F.; Fattorusso, C.; Catalanotti, B.; Aiello, F.; Gemma, S.; Nacci, V.; Novellino, E.; Stark, J. A.; Cagnotto, A.; Fumagalli, E.; Carnovali, F.; Cervo, L.; Mennini, T. Synthesis and pharmacological evaluation of potent and highly selective D_3 receptor ligands: inhibition of cocaine-seeking behavior and the role of dopamine D_3/D_2 receptors. *J. Med. Chem.* **2003**, *46*, 3822–3839.

(44) Campiani, G.; Butini, S.; Fattorusso, C.; Catalanotti, B.; Gemma, S.; Nacci, V.; Morelli, E.; Cagnotto, A.; Mereghetti, I.; Mennini, T.; Carli, M.; Minetti, P.; Di Cesare, M. A.; Mastroianni, D.; Scafetta, N.; Galletti, B.; Stasi, M. A.; Castorina, M.; Pacifici, L.; Vertechy, M.; Serio, S. D.; Ghirardi, O.; Tinti, O.; Carminati, P. Pyrrolo[1,3]benzothiazepine-based serotonin and dopamine receptor antagonists. Molecular modeling, further structure−activity relationship studies, and identification of novel atypical antipsychotic agents. *J. Med. Chem.* **2004**, *47*, 143–157.

(45) CVFF: Dauber-Osguthorpe, P.; Roberts, V. A.; Osguthorpe, D. J.; Wolff, J.; Genest, M.; Hagler, A. T. Structure and energetics of ligand binding to proteins: *E. coli* dihydrofolate reductase−trimethoprim, a drug−receptor system. *Proteins: Struct., Funct., Genet.* **1998**, *4*, 31–47.

(46) Fletcher, R. Unconstrained Optimization. In *Pratical Methods of Optimization*; John Wiley & Sons: New York, 1980; Vol. 1.

(47) (a) Stewart, J. J. P. MOPAC: a semiempirical molecular orbital program. *J. Comput.-Aided Mol. Des.* **1990**, *4*, 1–105. (b) Stewart, J. J. P. *MOPAC2007*; Stewart Computational Chemistry: Colorado Springs, CO, 2007; HTTP://OpenMOPAC.net.

(48) Tallarida, R. J.; Murray, R. B. *Manual of Pharmacologic Calculations with Computer Programs*, 2nd ed.; Springer-Verlag: New York, 1987.

(49) Motulsky, H.; Christopoulos, A. Fitting Models to Biological Data Using Linear and Non Linear Regression. www.GraphPad.Com, 2003.

(50) Motulsky, H. Statistic Guide: Statistical Analysis for Laboratory and Clinical Research: A Pratical Guide to Curve Fitting. www.GraphPad.com, 2003.

(51) Arunlakshana, D.; Schild, H. O. Some quantitative uses of drug antagonists. *Br. J. Pharmacol.* **1959**, *14*, 48–58.

(52) Tallarida, R. J.; Cowan, A.; Adler, M. W. pA_2 and receptor differentiation: a statistical analysis of competitive antagonism. *Life Sci.* **1979**, *25*, 637–654.

JM900018B